Discovery and optimization of non-steroidal FXR agonists from natural product-like libraries†

K. C. Nicolaou,*[a,b] Ronald M. Evans,[c] A. J. Roecker,[a] Robert Hughes,[a] Michael Downes[c] and Jeffery A. Pfefferkorn[a]

[a] *Department of Chemistry and The Skaggs Institute for Chemical Biology, The Scripps Research Institute, 10550 North Torrey Pines Road, La Jolla, 92037, California*

[b] *Department of Chemistry and Biochemistry, University of California San Diego, 9500 Gilman Drive, La Jolla, 92093, California*

[c] *Howard Hughes Medical Institute, The Salk Institute of Biological Sciences, 10010 North Torrey Pines Road, La Jolla, 92037, California*

The efficient regulation of cholesterol biosynthesis, metabolism, acquisition, and transport is an essential component of lipid homeostasis. The farnesoid X receptor (FXR) is a transcriptional sensor for bile acids, the primary product of cholesterol metabolism. Accordingly, the development of potent, selective, small molecule agonists, partial agonists, and antagonists of FXR would be an important step in further deconvoluting FXR physiology. Herein, we describe the development of four novel classes of potent FXR activators originating from natural product-like libraries. Initial screening of a 10 000-membered, diversity-orientated library of benzopyran containing small molecules for FXR activation utilizing a cell-based reporter assay led to the identification of several lead compounds possessing low micromolar activity (EC_{50}'s = 5–10 μM). These compounds were systematically optimized employing parallel solution-phase synthesis and solid-phase synthesis to provide four classes of compounds that potently activate FXR. Two series of compounds, bearing stilbene or biaryl moieties, contain members that are the most potent FXR agonists reported to date in cell-based assays. These compounds may find future utility as chemical tools in studies aimed at further defining the physiological role of FXR and discovering potential therapeutic agents for the treatment of diseases linked to cholesterol and bile acid metabolism and homeostasis.

Introduction

The efficient regulation of cholesterol biosynthesis, metabolism, acquisition and transport is an essential function of mammalian cells. High levels of cholesterol are associated with atherosclerosis, a leading cause of death in the western world and a major risk factor correlated with the occurrence of coronary heart disease and stroke. Until recently, recommendations for the treatment of hypercholestemia were focused on the use of statins, which inhibit the *de novo* biosynthesis of cholesterol, and the use of bile acid sequestering agents.[1] While statin-based agents are still in widespread use as cholesterol-lowering drugs, an understanding of the mechanisms controlling cholesterol homeostasis is evolving, and this has led to new molecular targets as candidates for therapeutic intervention.

Cholesterol metabolism is controlled through a complex feedback loop involving cholesterol itself and bile acids, which are cholesterol's primary oxidation products and, through secretion in the gut, the single most critical regulators of cholesterol absorption. The nuclear receptors LXR (liver X receptor) and FXR (farnesoid X receptor) are the specialized sensors for cholesterol and bile acids, respectively, that control transcription of networks encoding key metabolic enzymes.[2–5] For example, activation of LXR by oxysterols (*i.e.* mono-oxygenated cholesterol metabolites) leads to the up-regulation of CYP7A1, the enzyme that catalyzes the rate limiting step in the conversion of cholesterol to bile acids. In turn, bile acids[6–8] such as chenodeoxycholic acid (CDCA, **1**, Fig. 1) are ligands for FXR whose activation leads to a down-regulation of CYP7A1
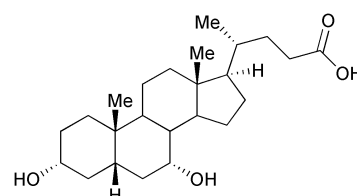
1: CDCA (low affinity endogenous agonist)
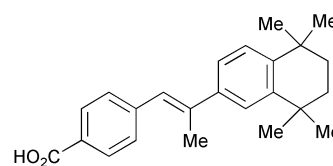
2: TTNPB (low affinity agonist; $EC_{50} > 1$ μM)
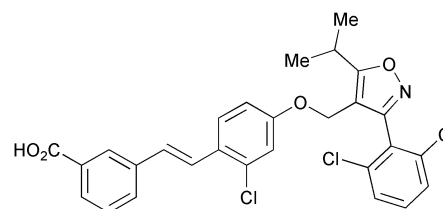
3: GW 4064 (high affinity agonist; $EC_{50} = 80$ nM)[a]

Fig. 1 Natural and synthetic agonists of FXR (farnesoid X receptor). [a]Cell-based assay.

leading to the completion of the feedback circuit. In this circuit FXR induces the expression of a transcriptional repressor SHP (small heterodimer partner) which, in turn, binds to LRH-1

(liver receptor homolog), required in CYP7A1 activation.[9,10] Additionally, both LXR and FXR are implicated in the regulation of several other gene products involved in cholesterol absorption, metabolism and transport.[11–17]

Thus, potent, selective, small molecule FXR agonists, partial agonists and antagonists would be powerful tools and would have many potential applications.[18] First, such compounds would facilitate the analysis of FXR physiology *in vivo*. Second, such compounds in conjunction with DNA arraying technology might allow for the discovery of new gene products under the control of FXR. Third, FXR modulators might find potential utility in the treatment of cholestasis and other disease states associated with aberrant levels, flow and release of bile acids. Fourth, in the absence of a crystal structure of FXR, a thorough SAR study of ligands that modulate the activity of FXR would allow for the delineation of the structural requirements for ligand binding and might aid in the design of future ligands and potential therapeutics.

As there is only one class of high affinity, non-steroidal agonists for FXR, exemplified by GW4064[19,20] (**3**, Fig. 1), our strategy for discovering similarly potent compounds was initiated with the screening of a 10 000-membered library constructed around the privileged 2,2-dimethylbenzopyran scaffold. Such privileged structures are attractive starting points for lead discovery, particularly when little or no structural information exists regarding the target, as they show good binding affinity toward a wide variety of enzymes and receptors.[21–23] Indeed, we have been able to use this library as a starting point for the successful discovery of potent inhibitors of NADH: Ubiquinone oxidoreductase[24] and for the identification and optimization of novel antibacterial agents.[25] The initial hits discovered from screening this library for FXR activation could be further optimized for potency and pharmacological properties suitable for the applications mentioned above. Herein, we describe the implementation of such a strategy culminating in the discovery of four classes of potent and selective activators of FXR.

Results and discussion

Previous screening technologies for identifying small molecule activators of FXR utilized a fluorescence resonance energy transfer (FRET) assay to detect the ligand-dependent recruitment of the coactivator SRC-1 to FXR.[26] The association of FXR with a coactivator is a necessary event for transcriptional activation. In the present investigations, however, we employed a cell-based transcription assay in which an FXR responsive promoter is linked to a luciferase reporter as our primary screen. In addition to ensuring that only cell permeable compounds were selected for further optimization, this approach allows for the detection of FXR activation in a natural system (*i.e.* correct folding of the protein and in the presence of a complete compliment of coactivators and corepressors).[27,28] Initial screening of a 10 000-membered combinatorial library of benzopyran-based small molecules in this high-throughput, cell-based assay for FXR activation produced several lead compounds whose structures are listed in Fig. 2a (**4**–**15**). Guided by the preliminary SAR gained from the evaluation of this initial library we designed and synthesized a follow-up focused library of *ca.* 200 benzopyran-based compounds on solid support (see Supplementary Scheme 1†). A selection of the most active compounds, possessing EC_{50} values between 5 and 10 μM, discovered from this second round of screening is shown in Fig. 2b (**16**–**27**). Compounds **26** and **27** proved to be among the most active at this stage and were the subject of further optimization as described below.

With initial lead compounds identified and validated, the stage was set for the systematic optimization of the three regions of the lead structure shown in Fig. 3. As detailed in the following sections, focused libraries were synthesized and screened in the cell-based assay in order to evaluate the structural requirements of each region of the molecule for potent FXR agonism. At this point we chose to utilize parallel solution-phase chemistry for the construction of additional focused libraries. This shift away from solid-phase chemistry provided us with maximum flexibility as we sought to rapidly and systematically optimize each region of the lead molecules using smaller designed libraries.

### Evaluation of benzopyran Region I SAR

Most of the FXR agonists reported to date including CDCA (**1**), TTNPB (**2**) and GW4064 (**3**) (see Fig. 1) contain a carboxylic acid moiety. We, thus, reasoned that incorporation of an acid unit within either Region I, II or III of structure **26** (Fig. 3) would confer increased potency upon this rather weak ligand (5–10 μM) identified *via* high throughput screening (HTS). Guided by this reasoning, we evaluated the SAR of Region I. Several compounds displaying the acid unit in various positions were synthesized (*e.g.* compounds **28**, **36**, **52**, **54** and **56**, Fig. 4) and tested. None of these compounds, however, showed improved activation of FXR. Interestingly, compound **29**, bearing a *meta* methyl acrylate moiety, was a substantially better activator of FXR than compound **26**. The preparation of compound **29** is representative of the methods employed to construct these compounds and is described in Scheme 1 (see Supplementary Schemes 2–4† for further experimental procedures). Thus, aldehyde **59** was selectively methylated[29] (NaH, MeI), alkylated (2-methyl-3-butyn-2-ol, TFAA, DBU, CuCl₂), reduced (Lindlar, H₂) and thermally cyclized to yield benzopyran **60**. Reductive amination of aldehyde **60** with 3-bromoaniline (NaCNBH₃) followed by acylation with cyclopropanecarbonyl chloride (C₃H₅COCl, Et₃N) and palladium-mediated Heck coupling (Pd₂(dba)₃, P(*o*-tol)₃, Et₃N) with methyl acrylate provided **29**.
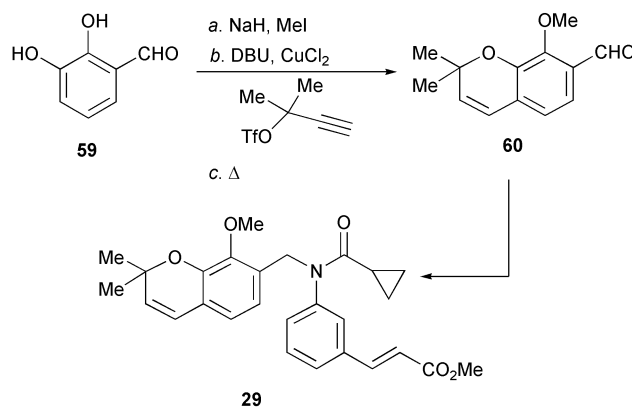

Scheme 1 Representative procedure for the preparation of Region I modified compounds: synthesis of methyl acrylate **29**. *Reagents and conditions*: (a) see ref. 28; (b) 1.5 equiv. 2-methyl-3-butyn-2-ol, 1.5 equiv. DBU, 1.7 equiv. trifluoroacetic anhydride, 0.1 equiv. CuCl₂, CH₃CN, 0 → 25 °C, 12 h, 75%; (c) *N*,*N*-diethylaniline, 190 °C, 0.5 h, 90%; (d) 1.5 equiv. 3-bromoaniline, THF, 70 °C, 4 h; then 2.0 equiv. NaCNBH₃, 10% MeOH, 70 ° C, 4 h, 83%; (e) 1.3 equiv. cyclopropanecarbonyl chloride, 1.3 equiv. Et₃N, 0.1 equiv. 4-DMAP, CH₂Cl₂, 25 °C, 12 h, 90%; (f) 4.0 equiv. methyl acrylate, 0.2 equiv. Pd₂(dba)₃, 0.5 equiv. P(*o*-tol)₃, 5.0 equiv. Et₃N, DMF, 90 °C, 24 h, 80%. DBU = 1,8-diazabicyclo[5.4.0]undec-7-ene, 4-DMAP = 4-dimethylaminopyridine, Pd₂(dba)₃ = tris(dibenzylideneacetone)dipalladium(0).

In further refining the SAR of Region I, an important observation was that the location of the methyl acrylate moiety at the *meta* position was crucial for potent activation of FXR as compound **53** (Fig. 4) bearing a *para* methyl acrylate does not activate FXR. In order to further examine what functionality was tolerable at the *meta* position, we synthesized the additional compounds shown in Fig. 4. From biological screening
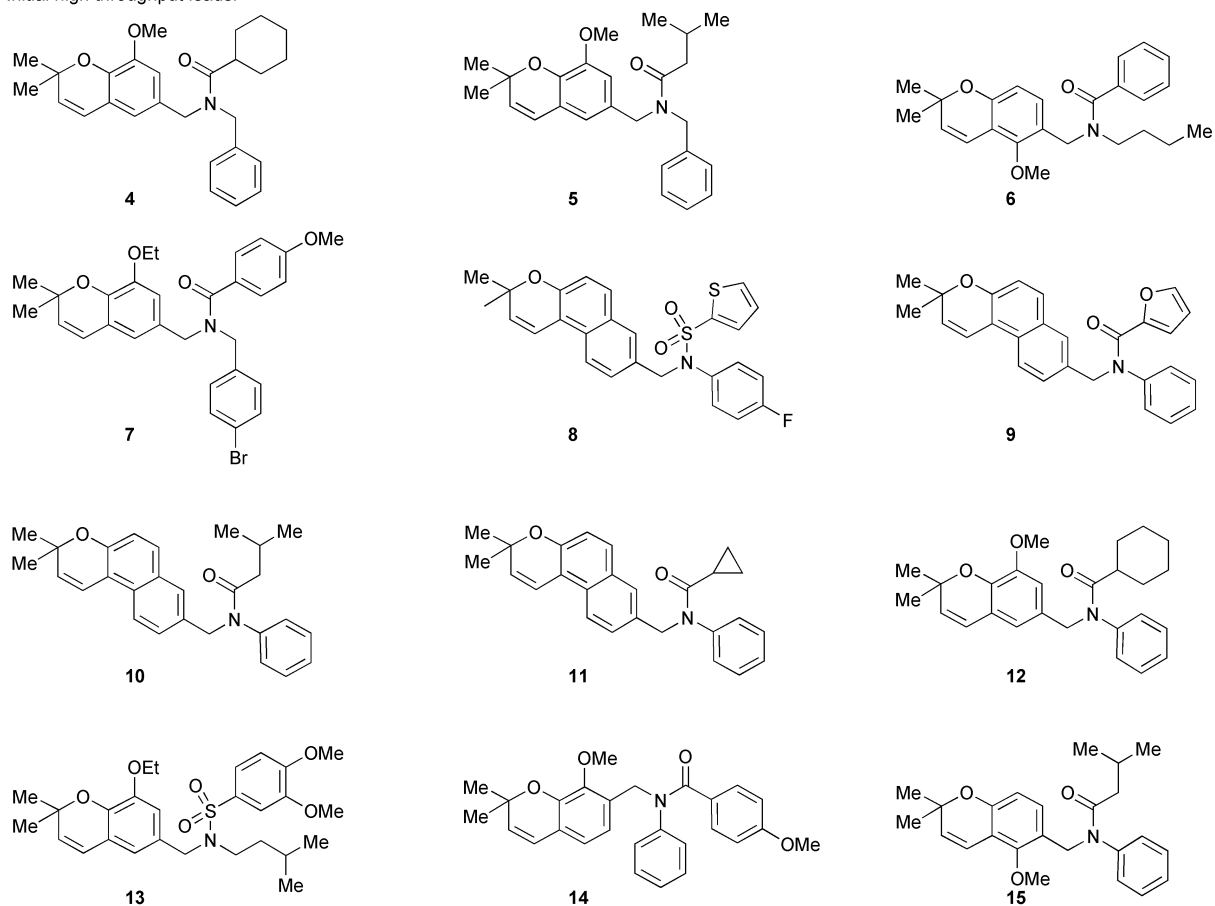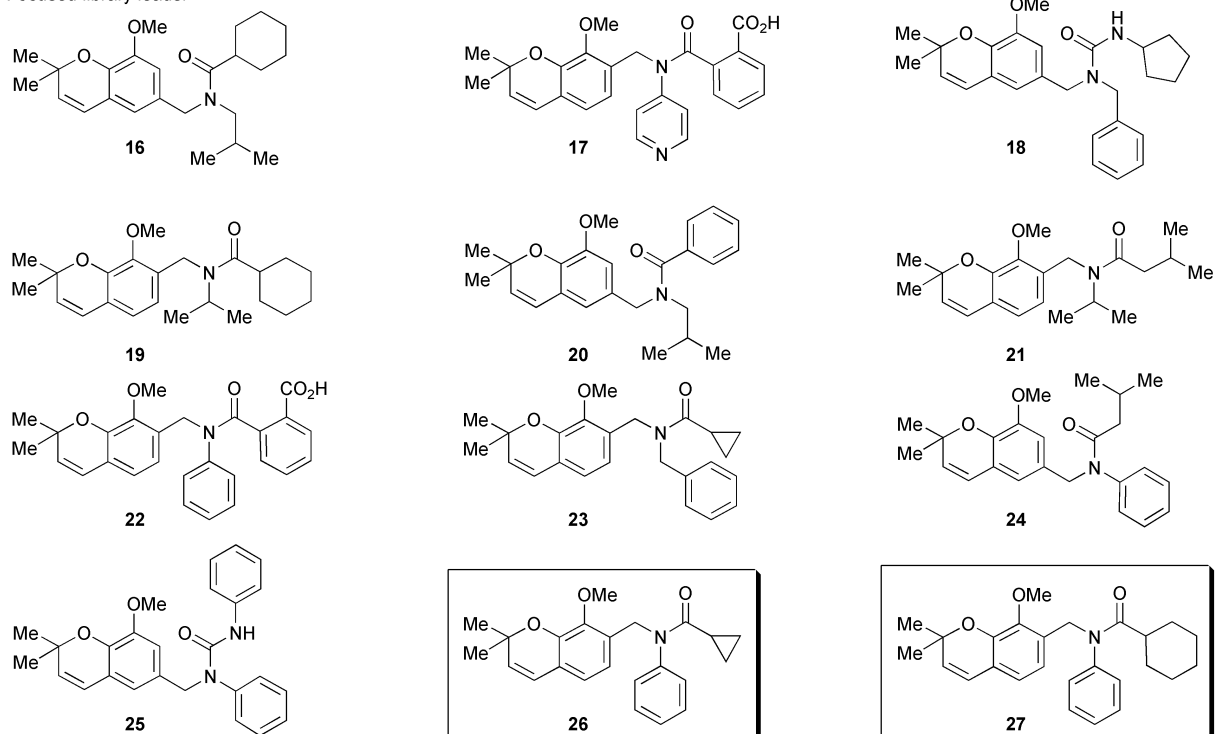
Fig. 2 a) Selected hits from a high throughput screen for FXR agonism of a 10,000-membered benzopyran-based natural product-like library (EC_{50} = 5–10 μM). b) Selected low affinity FXR agonists from follow-up solid phase benzopyran library (EC_{50} = 5–10 μM). See Supplementary Scheme 1 † for details of the focused library synthesis. The boxed compounds represent the most potent FXR agonists.

of these compounds it became clear that the length and rigidity of the tether between the aromatic core and the interacting functionality (either methyl ester or methyl ether) are important

for FXR agonism. For instance, compounds **41** and **45** appear to possess either too short or too long of a tether for potent activity; compounds **35** and **46–49** presumably cannot adopt
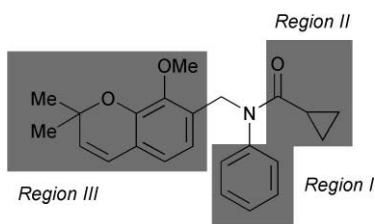
Fig. 3 Selected regions of interest for SAR evaluation of lead compound **26**. Region I: right-hand aromatic system; Region II: acyl group region; Region III: left-hand benzopyran ring system.

the correct orientation for potent activation; and compounds **30**, **31**, **34**, **38**, **39**, **40**, and **50** do not apparently present the correct interacting functionality to the receptor as they are inactive. Indeed, of all the analogs designed to probe the SAR of Region I, only compounds **29** and **33** are capable of activating FXR to a significant extent. Due to relative ease of synthesis of compound **29** we chose to use this analog as a starting point for the optimization of Region II.

Evaluation of benzopyran Region II SAR

As shown in Fig. 5, we examined the effect of numerous sub-

stitution patterns in this region of the molecule (see Supplementary Scheme 5† for preparation of these compounds). Only compounds **65** (EC_{50} = 358 nM) and **68** (EC_{50} = *ca.* 1 μM) were more effective than compound **29** in activating FXR. Substituted aromatic amide derivatives such as **69–77** were all found to be less active than the parent compound **68**. Alkyl derivatives **78** and **79** were inactive as were sulfonamide **82**, thiourea **84**, and thioamide **83** suggesting the importance of acylation at this position. The sum of these results pointed to Region II requiring moderately bulky cycloalkyl amide moieties for optimal activity.

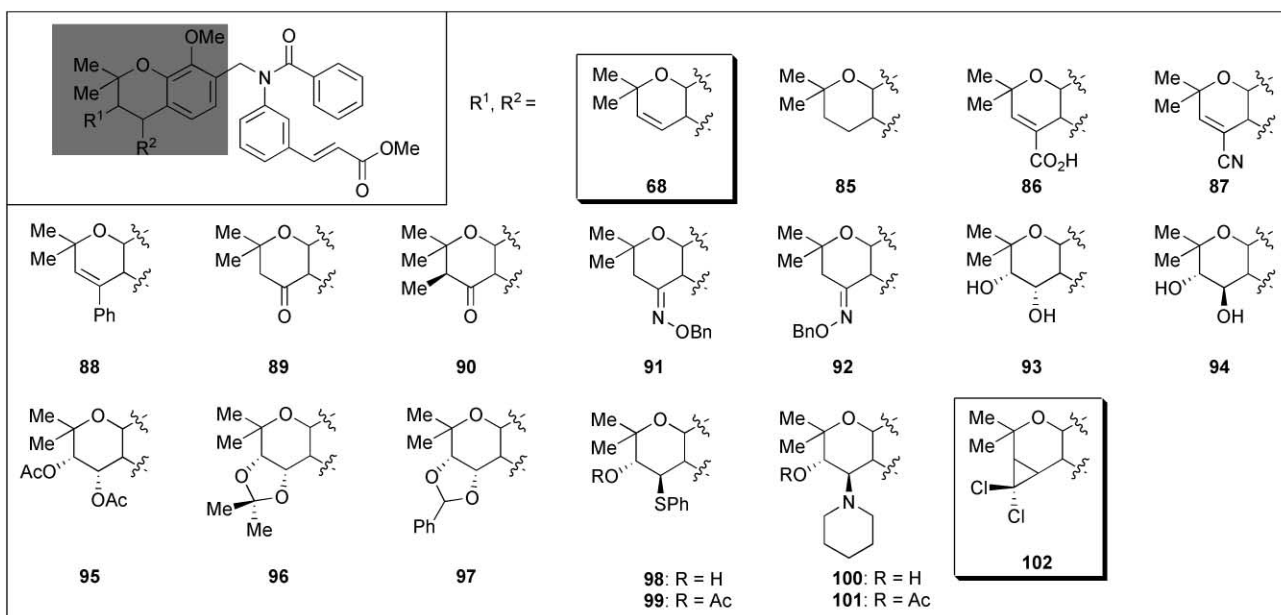### Evaluation of benzopyran Region III SAR

Having thoroughly examined Regions I and II, we then turned our attention to the optimization of Region III (see Fig. 6 for structures and Supplementary Schemes 6 and 7† for preparation of compounds). Incorporation of polar H-bond donating functional groups such as those that adorn compounds **86**, **93**, **94**, **98** and **100** did not improve the activity of the analogs. Nor did the addition of H-bond acceptors such as in **89**, **90**, **95**, **99** and **101** improve the ability of the parent compound **68** to activate FXR. Finally, the addition of bulky lipophilic groups to the benzopyran moiety afforded compounds that
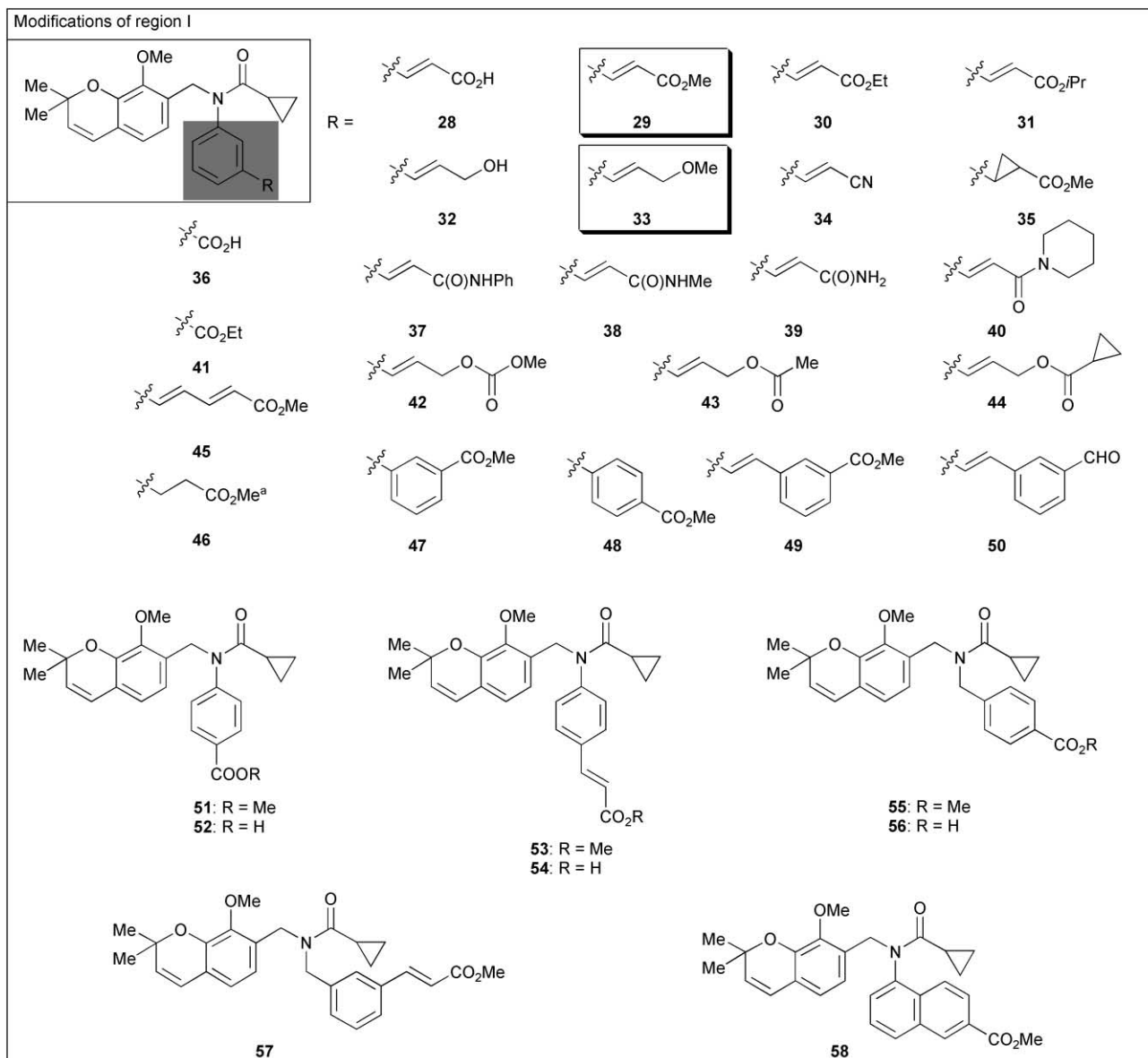
Fig. 4 Examination of Region I SAR. See Scheme 1 and Supplementary Schemes 2–4† for a description of the synthesis of these compounds.
[a] Benzopyran double bond is also saturated in this compound. Boxed compounds represent the most potent FXR agonists.
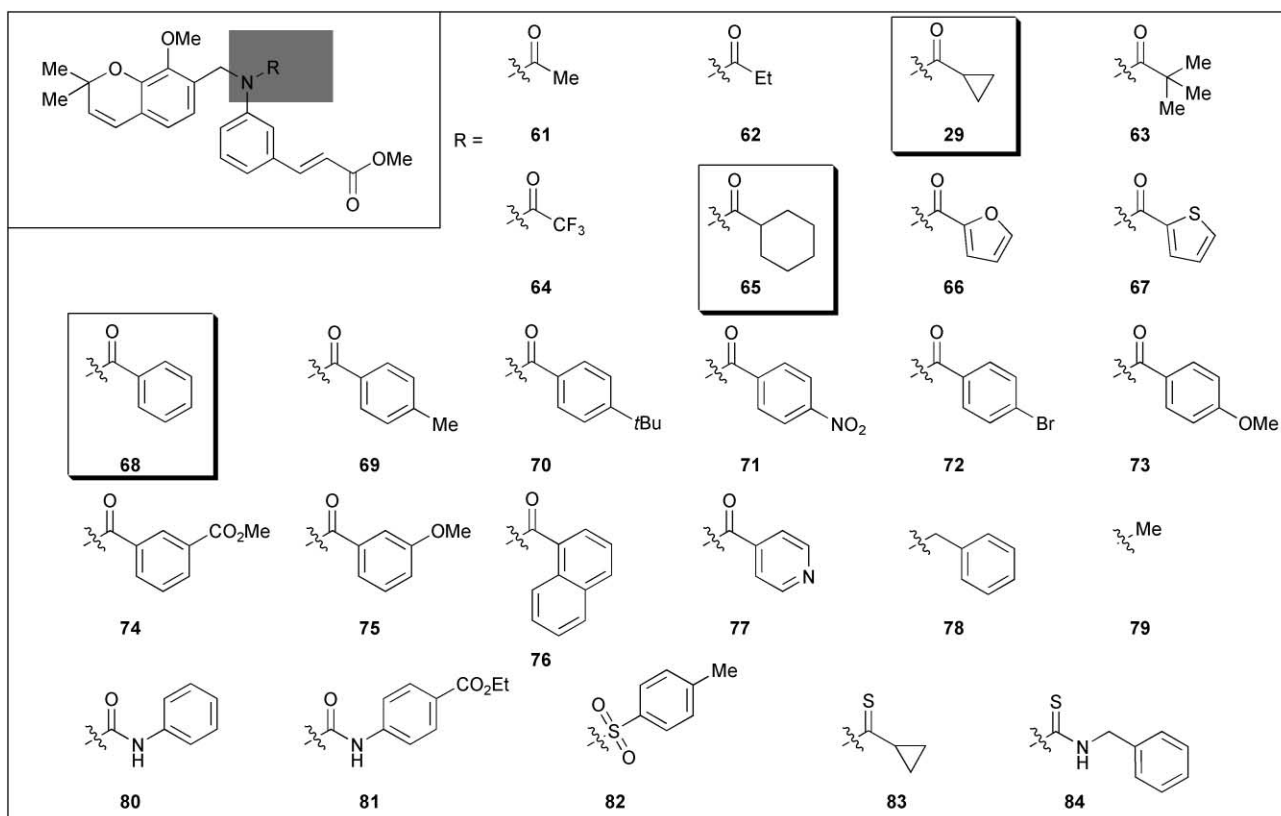
Fig. 5 Examination of the acyl group (Region II) SAR. See Supplementary Scheme 5† for a description of these compounds. Boxed compounds are the most active FXR agonists.
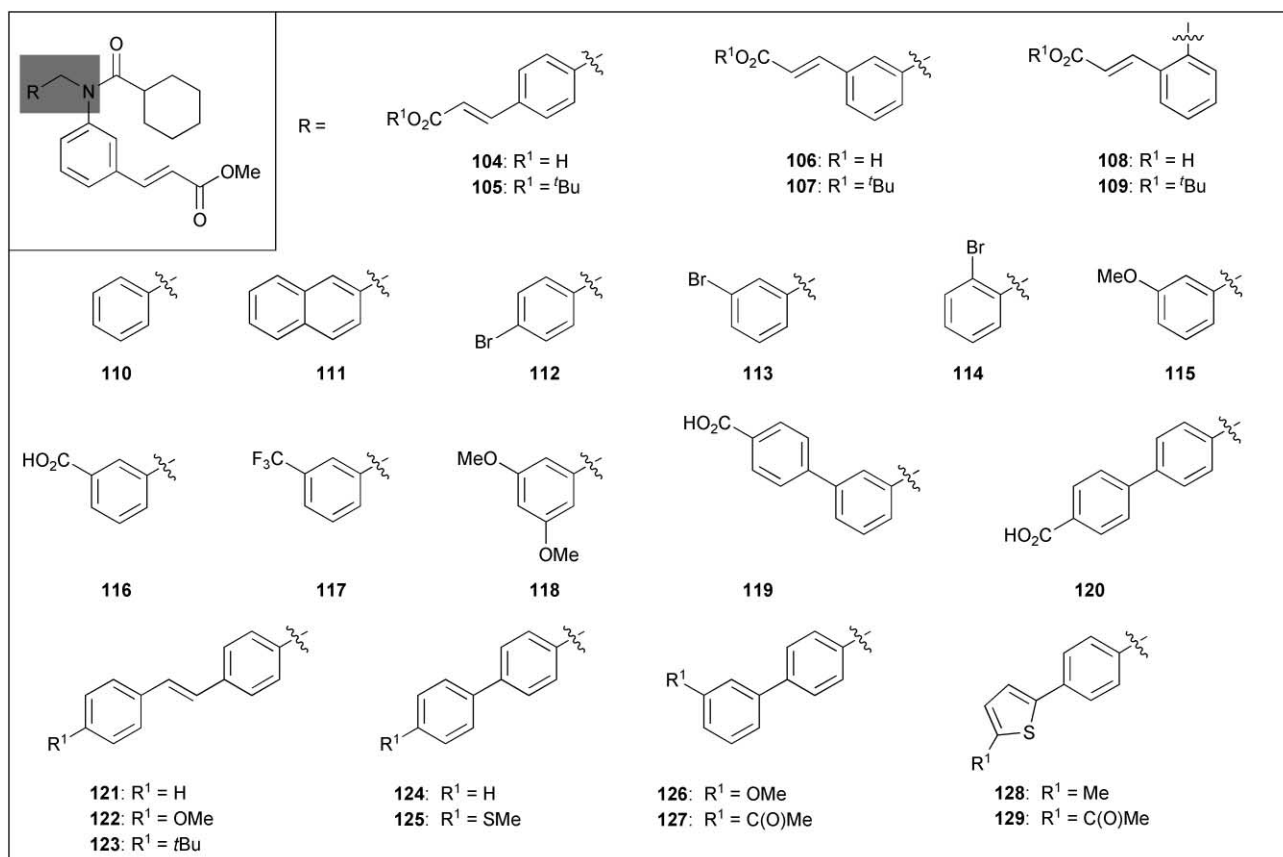

Fig. 6 Examination of the benzopyran (Region III) SAR. See Scheme 2 and Supplementary Schemes 6 and 7† for a description of the synthesis of these compounds. Boxed compounds are the most active FXR agonists.

only weakly activated FXR. However, replacement of the double bond in the benzopyran unit by a dichlorocyclopropane unit provided analog **102** (EC_{50} = 333 nM). This potent compound was synthesized as depicted in Scheme 2. Thus, benzopyran **103** was cyclopropanated under phase transfer conditions (adogen 464 (cat), NaOH, CHCl$_3$) and converted to the corresponding cinnamate *via* a Heck coupling (Pd$_2$(dba)$_3$, P(o-tol)$_3$, Et$_3$N) with methyl acrylate to yield **102**. Replacement of the benzoyl group in Region II of compound **102** with the cyclohexanecarbonyl moiety afforded the even more potent compound **149** (EC_{50} = 188 nM) (Table 1c).

Although compound **149** (EC_{50} = 188 nM) represents a significant improvement in potency over compound **65** (EC_{50} = 358 nM), it became clear that further possibilities for optimization of this class of compounds were limited. Therefore, we chose to examine the effect of replacing the benzopyran moiety with other ring systems.

Fig. 7 presents a set of compounds in which the benzopyran moiety was replaced with certain groups of varying molecular diversity (see Supplementary Schemes 8 and 9† for preparation). Biological assays showed that replacement of the benzopyran with a small aromatic unit generally had a detrimental effect on activity. For instance, compounds **110** and **112**–**117** (see Table 1c and Fig. 7) were inactive, while compounds **111** and

Fig. 7 Examination of the benzopyran replacement (Region III) SAR. See Scheme 3 and Supplementary Schemes 8, 9 and 10† for a description of the synthesis of these compounds.
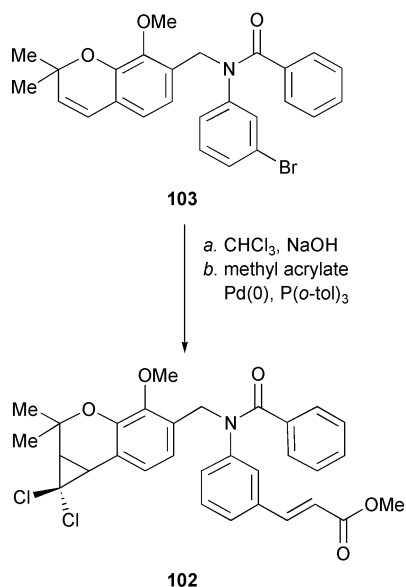
Scheme 2 Synthesis of compound **102**. Exploration of Region III SAR. *Reagents and conditions*: (a) CHCl₃–2.0 M NaOH (7 : 1), adogen 464 (cat.), 25 °C, 6 h, 85%; (b) 2.0 equiv. methyl acrylate, 0.2 equiv. Pd₂(dba)₃, 0.6 equiv. P(o-tol)₃, 5.0 equiv. Et₃N, DMF, 90 °C, 24 h, 75%. DMF = dimethylformamide.

118 showed only moderate activation of FXR (EC_{50} = 680 nM and 606 nM, respectively). However, replacement of the benzopyran with an aromatic ring bearing substituents at the *para* position produced compounds with improved activity. For example, 4-*tert*-butyl cinnamate **105** (EC_{50} = 127 nM), stilbenes **121** and **122** (EC_{50} = 36 and 208 nM, respectively), biaryls **124**–**127** (EC_{50} = 510, 69, 77, 227 nM, respectively) and aryl thiophenes **128** and **129** (EC_{50} = 206 and 256 nM, respectively)

were all potent activators of FXR in the cell-based reporter assay. The synthesis of compound **105** is outlined in Scheme 3 (see Supplementary Scheme 14† for the preparation of **121**–**129**). Thus, acylation of 3-bromoaniline (C₆H₁₁COCl, Et₃N) gave cyclohexylamide **131**. Subsequent reaction of **131** under Heck coupling conditions (Pd₂(dba)₃, P(o-tol)₃, Et₃N) with methyl acrylate gave **132**. Finally, alkylation (4-bromobenzyl bromide, NaH) of cinnamate **132** followed by a second Heck coupling (Pd₂(dba)₃, P(o-tol)₃, Et₃N) with *tert*-butyl acrylate gave **105**.

This initial survey of the three regions of SAR outlined in Fig. 3 led to the identification of four classes of potent FXR agonists (based on the differences in Region III substitution) for further evaluation. The first class is represented by benzopyran-derived dichlorocyclopropane **149** (EC_{50} = 188 nM). Compound **105** (EC_{50} = 127 nM) is the prototypical member of the bis-cinnamate series. Finally, compounds **121** (EC_{50} = 36 nM) and **124** (EC_{50} = 69 nM) are members of the stilbene and biaryl series, respectively. Based on data presented in Figs 4, 5 and 6, compound **149** (Table 1c) appeared to represent the optimal potency that could be readily obtained in the benzopyran-derived series. However, the bis-cinnamate, biaryl, and stilbene series were thought to still possess considerable potential for further development and rigorous SAR analysis. Below we detail the results of such investigations which indeed led to further enhancement of biological activity.

Examination of the bis-cinnamate series

Similar to the results described above, the *meta* substituted methyl cinnamate moiety on the "right-hand" region of the molecule remained a necessary component for optimal activity in the bis-cinnamate series (see Table 1a and Supplementary Scheme 11†). Replacement of this methyl acrylate unit with either a methyl or ethyl allylic ether (**136** and **137**) caused only a

Table 1 Panel a) Highlights of Region I SAR. Panel b) Highlights of Region II SAR in the bis-cinnamate series. Panel c) Effects of benzopyran substitution. Panel d) Highlights of Region III SAR including the bis-cinnamate, styryl and biaryl series. Values represent the mean of at least four experiments. RE = relative efficacy of the indicated compound at 1 μM to 100 μM CDCA.

a. SAR of region I

	R	EC$_{50}$ (nM)	RE[a]
105	COOMe	127	2.12
133	COOEt	256	2.07
134	COO^{t}Bu	>1000	1.06
135	CONH$_2$	>1000	0.50
136	CH$_2$OMe	243	1.68
137	CH$_2$OEt	220	1.74
138	CH$_2$OPh	2830	0.45

139: EC$_{50}$ = 274 nM
RE[a] = 1.38

b. SAR of region II

	R	EC$_{50}$ (nM)	RE[a]
140	cyclopropyl	250	1.68
141	cyclobutyl	187	1.84
142	cyclopentyl	162	2.16
105	cyclohexyl	127	2.12
143	phenyl	236	1.96
144	2-furyl	205	1.93
145	isopropylamino	212	1.96
146	benzylamino	>1000	0.27

c. SAR of region III

	R	EC$_{50}$ (nM)	RE[a]
132	H	>1000	0.09
147	methyl	>1000	0.09
110	benzyl	>1000	0.09
111	2- napthyl	680	0.41
114	2-bromobenzyl	>1000	0.11
113	3-bromobenzyl	>1000	0.10
112	4-bromobenzyl	>1000	0.28
148	4-tert-butylbenzyl	>1000	0.15
115	3-methoxybenzyl	>1000	0.11
118	3,5-dimethoxybenzyl	606	0.11
117	3-(trifluromethyl)benzyl	>1000	0.12

	R	EC$_{50}$ (nM)	RE[a]
68	phenyl	>1000	0.83
65	cyclohexyl	358	0.40

	R	EC$_{50}$ (nM)	RE[a]
102	phenyl	333	0.64
149	cyclohexyl	188	0.50

d. SAR of region III

	R	EC$_{50}$ (nM)	RE[a]
104	COOH	>1000	0.08
150	COOMe	>1000	0.87
151	COOEt	>1000	1.14
152	COO^{i}Pr	163	1.97
105	COO^{t}Bu	127	2.12
153	COOBn	>1000	0.23
154	CONMe$_2$	>1000	0.66
155	CONH^{t}Bu	>1000	1.65
156	CH$_2$OMe	233	1.63
157	CH$_2$OEt	198	2.06
158	CH$_2$OPh	>1000	0.64

	R	EC$_{50}$ (nM)	RE[a]
159	COOMe	240	1.56
160	COO^{t}Bu	>1000	0.64

	R	EC$_{50}$ (nM)	RE[a]
161	H	> 1000	0.12
162	Me	> 1000	0.14
163	Bn	> 1000	0.38
164	MeC(O)	> 1000	0.16
165	C$_6$H$_5$C(O)	> 1000	0.16
166	MeS(O$_2$)	> 1000	0.18
167	EtOOCCH$_2$	> 1000	0.18

	R^1	R^2	EC$_{50}$ (nM)	RE[a]
126	OMe	H	77	1.51
127	C(O)Me	H	227	1.30
125	H	SMe	69	1.74
124	H	H	510	0.71

	R	EC$_{50}$ (nM)	RE[a]
128	Me	206	1.78
129	C(O)Me	256	1.48

	R	EC$_{50}$ (nM)	RE[a]
121	H	36	1.55
122	OMe	208	1.67
123	t-Bu	>1000	0.29

slight decrease in activity (EC$_{50}$ = 243 and 220 nM, respectively). A marked decline in potency accompanied substitution of the methyl acrylate by more sterically bulky ethers or esters (133 and 134) or amides (135). Interestingly, saturation of the acrylate olefin (139) afforded only a two-fold decrease in potency, EC$_{50}$ = 274 nM, which supports the notion that conformational rigidity is a factor contributing to, but not essential for, high affinity ligands. Importantly, compound 139 suggests that the methyl acrylate moiety is not simply functioning as a latent electrophile.

Region II also closely mirrored the preceding data as cyclo-alkyl amides remained the optimal substituents (105 and 140–142: EC$_{50}$ = 127–250 nM) in the bis-cinnamate series (see Table 1b and Supplementary Scheme 12†). Aromatic and heterocyclic amides as well as alkyl ureas led to moderate potency (143–145: EC$_{50}$ = 205–236 nM) whereas incorporation

of bulky ureas such as in compound 146 rendered compounds of only marginal efficacy.

As mentioned above, replacement of the benzopyran moiety with a benzyl group bearing a tert-butyl acrylate moiety in the para-position yielded compound 105 with dramatically increased efficacy (EC$_{50}$ = 127 nM). Interestingly, placement of the same tert-butyl acrylate group in either the meta or ortho positions of the aromatic ring (107 and 109, Fig. 7 and Supplementary Scheme 9† for synthesis) in Region III led to only micromolar potency. Further investigation of the "left-hand" region in this series of compounds demonstrated that a decrease in ester group size yielded a corresponding decrease in efficacy (EC$_{50}$ of t-butyl > i-propyl > ethyl > methyl; compounds 105, 150–152, Table 1d and Supplementary Scheme 10†). Similarly, substitution of the ester with either carboxylic acid or amide functionality provided less effective compounds
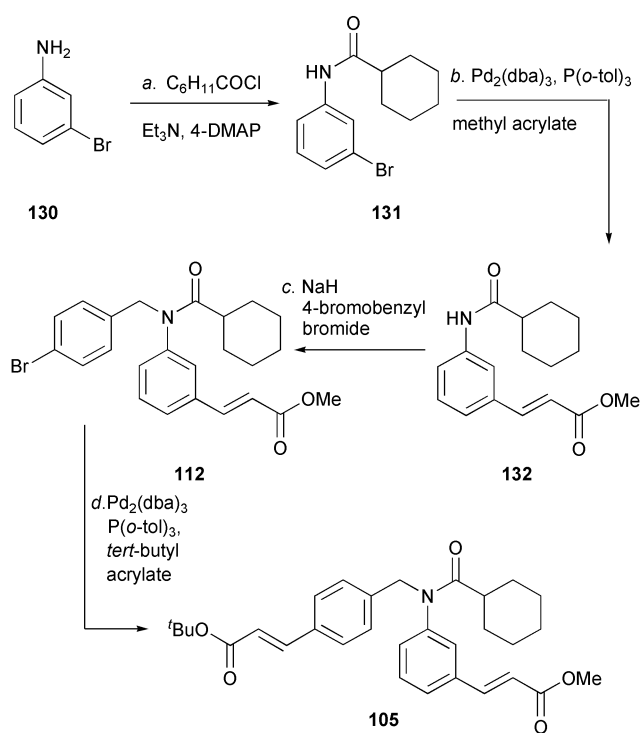
Scheme 3 Preparation of bis-cinnamate **105**. *Reagents and conditions*: (a) 1.1 equiv. $C_6H_{11}COCl$, 1.3 equiv. Et_3N, 0.05 equiv. 4-DMAP, CH_2Cl_2, 25 °C, 3 h, 95%; (b) 4.0 equiv. methyl acrylate, 5.0 equiv. Et_3N, 0.2 equiv. $Pd_2(dba)_3$, 0.6 equiv. $P(o\text{-tol})_3$, DMF, 90 °C, 12 h, 80%; (c) 1.1 equiv. NaH, THF, 0 °C, 30 min; then 1.3 equiv. 4-bromobenzyl bromide, THF, 0 °C, 2 h, 90%; (d) 4.1 equiv. acrylate, 5.0 equiv. $Pd_2(dba)_3$, 0.15 equiv. $P(o\text{-tol})_3$, DMF, 90 °C, 12 h, 75%.

with EC_{50} values in the micromolar range. Substitution of the *tert*-butyl acrylate moiety with a methyl or ethyl allylic ether (**156** and **157**) retained considerable potency (EC_{50} = 233 and 198 nM, respectively). However, the more bulky phenyl allylic ether **158** possessed only micromolar activity. In addition, saturation of the acrylate moiety (**159**) showed a two-fold decrease in potency from the parent compound (**105**). Finally, substitution of the *ortho* position of the aromatic ring of the *tert*-butyl acrylate series with oxygenated functionality (**161–167**, see Table 1d and Supplementary Scheme 13† for synthesis) afforded compounds with very low biological activity.

Construction of biaryl and stilbene containing focused libraries

In an effort to further optimize the biaryl and stilbene series, a 93-membered library of such compounds was constructed employing a split-and-pool solid phase strategy. Individual library members were identified *via* radiofrequency encoding using IRORI™ tags and MacroKan™ technologies.[21–23] As shown in Scheme 4, Boc protected cinnamic acid **168** was immobilized on Merrifield resin (Cs_2CO_3) to afford resin **169**. The Boc group of this resin was removed by treatment with 20% TFA in CH_2Cl_2 and the resultant resin-bound amine was reductively alkylated with 4-bromobenzaldehyde ($NaCNBH_3$) to yield amino resin **170**. Resin **170** was acylated with one of three acyl groups to give amide or urea resins **171**. The acylated resins (**171**) were subjected to either Heck coupling ($Pd_2(dba)_3$, $P(o\text{-tol})_3$, Et_3N) with thirteen substituted styrenes or Suzuki coupling ($Pd(PPh_3)_4$, Cs_2CO_3) with eighteen boronic acids to yield stilbene resins **172** and biaryl resins **173**, respectively. In selecting appropriate styrenes and boronic acids for inputs into this combinatorial library we were guided by initial comparisons of *tert*-butyl stilbene (**123**, EC_{50} = >1000 nM) to the unsubstituted stilbene **102** (EC_{50} = 36 nM), and biaryl compound **124** (EC_{50} = 510 nM) to **125** (EC_{50} = 69 nM) as shown in Table 1. We reasoned that both the stilbene and the biaryl ligands needed to fit into the same region of space within the

receptor site for potent activation. Hence, stilbenes in which the aromatic nucleus is removed two carbon atoms further away from the core of the molecule should be adorned with small substituents while the biaryl compounds should be substituted with larger functionality for optimal activity. Cleavage of resins **172** and **173** with NaOMe yielded methyl acrylates **121,125,126** and **174–264**. Analysis of the library by LCMS after purification (PTLC) showed the average purity of these compounds to be >95%.

Screening of this compound library in the cell-based assay led to some intriguing results as summarized in Table 2. Thus, it was found that in both the stilbene and biaryl series, analogs bearing the cyclohexyl amide moiety are generally the most potent followed by those bearing the isopropyl amide or isopropyl urea units. As expected, stilbenes bearing smaller substituents were more potent than those carrying larger functionality. For instance, unsubstituted stilbene **121** and mono-fluoro stilbenes **192**, **200**, and **203** were among the most active, while mono-methyl derivative **174** and tri-methyl derivative **195** were among the least active. Also of interest were the heterocyclic compounds **207** and **210** which retained good potency (EC_{50} = 309 and 227 nM, respectively) and may possess improved pharmacological properties. In the biaryl series, compounds which present more bulky substituents at the terminus of the structure were more active. In this series, compounds **259** (EC_{50} = 25 nM) and **244** (EC_{50} = 38 nM) were particularly active. Overall, most of the compounds synthesized in this follow-up study were efficient activators of FXR, providing further support for our working hypothesis for the FXR binding pocket, as described above. This model may provide a solid basis for further development of FXR activators.

A summary of the molecular requirements for potent FXR activation is shown in Fig. 8. Thus, in Region I the presence of the *meta* methyl acrylate unit is important for potent activation as only a few modifications retain good activity. The most potent compounds possess a cycloalkylamide in Region II. Finally, Region III is the most tolerant and several structural elements were found to provide a good fit within the pocket of the receptor.
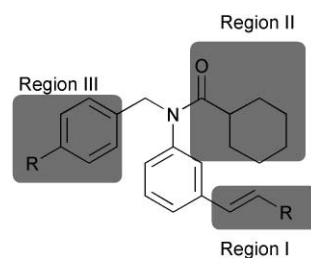

Fig. 8 Summary of structural requirements for potent FXR activation. Region I: methyl acrylate or allylic methyl ether necessary for optimum activity. In some instances, when other areas were optimized, olefin can be removed while retaining some potency. Region II: amide or urea essential for maximum activity. Alkyl or cycloalkyl amide or urea affords most potent compounds. Region III: must have *para*-position functionalized for activity. Steric bulk and length seem to be the most important factors which govern potency. This region is tolerant of many different structural motifs.

In order to determine how selectively the compounds above activated FXR we screened some of the most active compounds against a panel of nuclear receptors and the full details of this cross-activation screening will be reported elsewhere.[30] It suffices to note here that most of these compounds were found to be highly selective, activating only FXR. Notably, however, compound **149** also potently activated SXR (FXR: EC_{50} = 188 nM, SXR: EC_{50} = 77 nM). Far from being discouraging, this result may lead to compounds which may find utility in the treatment of diseases linked to the accumulation of toxic bile acids.[31,32]
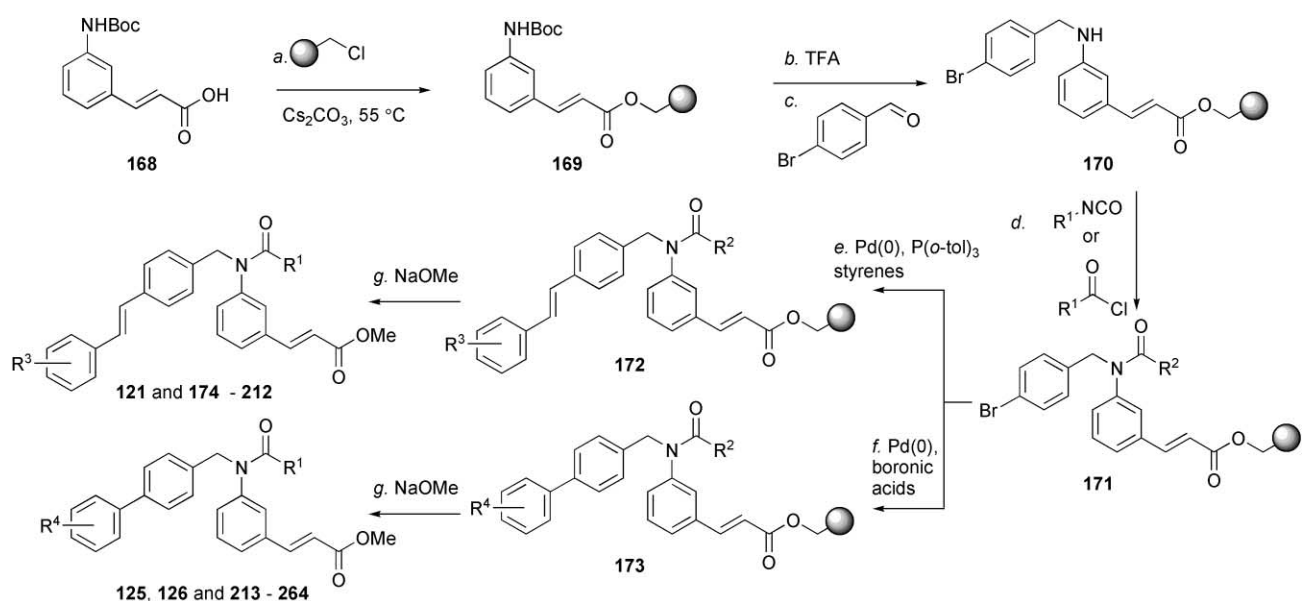
Scheme 4 Solid phase synthesis of focused libraries of biaryl and stilbene cinnamates. *Reagents and conditions*: (a) 2.0 equiv. **168**, 1.0 equiv. Merrifield resin (0.91 mmol g^{-1}), 2.0 equiv. Cs$_2$CO$_3$, 0.5 equiv. TBAI, DMF, 55 °C, 24 h; (b) 20% TFA in CH$_2$Cl$_2$, 25 °C, 1 h; (c) 10.0 equiv. 4-bromobenzaldehyde, 0.05 equiv. AcOH, THF–MeOH (2 : 1), 25 °C, 1 h; then, 8.0 equiv. NaCNBH$_3$, THF–MeOH (2 : 1), 25 °C, 2 h; (d) for R^{1}C(O)Cl: 30.0 equiv. i-PrC(O)Cl or C$_6$H$_{11}$C(O)Cl, 40.0 equiv. Et$_3$N, 1.0 equiv. 4-DMAP, CH$_2$Cl$_2$, 25 °C, 12 h; for R^{1}NCO, 30.0 equiv. i-PrNCO, 40.0 equiv. Et$_3$N, 1.0 equiv. 4-DMAP, DMF, 65 °C, 60 h; (e) 8.0 equiv. styrene, 10.0 equiv. Et$_3$N, 0.5 equiv. Pd$_2$(dba)$_3$, 1.5 equiv. P(*o*-tol)$_3$, DMF, 90 °C, 48 h; (f) 5.0 equiv. boronic acid, 3.0 equiv. Cs$_2$CO$_3$, 0.5 equiv. Pd(PPh$_3$)$_4$, DMF, 90 °C, 24 h; (g) 10.0 equiv. NaOMe, Et$_2$O–MeOH (10 : 1), 25 °C, 20 min. TBAI = tetrabutylammonium iodide, TFA = trifluoroacetic acid.
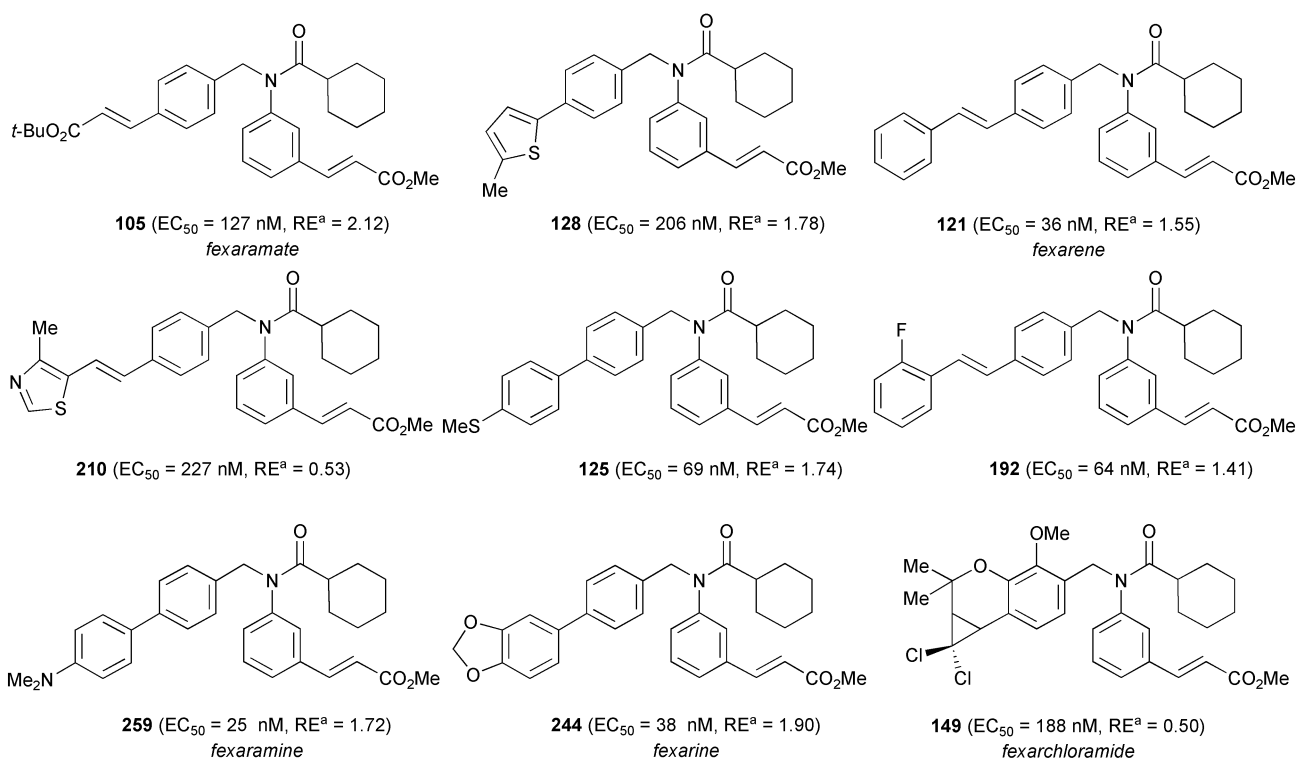
Fig. 9 Lead compounds (and their EC$_{50}$ values in a cell-based assay) selected for further biological evaluation as FXR agonists. *[a]* RE = relative efficacy of the indicated compound at 1 μM to 100 μM CDCA.

Conclusion

In this article we describe work which demonstrated the utility of natural product-like libraries as fertile pools for the discovery of novel FXR agonists. This study has produced, as summarized in Fig. 9, four diverse classes of FXR agonists, several of which are among the most potent FXR activators reported to date. To facilitate future reference to these compounds we propose to name them as follows: **105** as fexaramate, **121** as fexarene, **259** as fexaramine, **244** as fexarine and **149** as fexarchloramide. In addition to the discovery of potent compounds, the complete investigation of the SAR of these families of compounds may facilitate further optimization of additional desired properties for these agonists. It is interesting to note that none of these potent compounds, in contrast to the previously reported FXR agonists (see Fig. 1), contains a carboxylic acid moiety. Studies are currently under way to elucidate the potential structural significance of this observation. Additionally, ongoing biological studies utilizing this expanded repertoire of orphan receptor ligands specifically activating FXR are aimed at further elucidating the physiological function of this newly discovered receptor. Finally, some of these compounds may

	R¹	R²	R³	R⁴	R⁵	R⁶	EC₅₀ (nM)	REᵃ
174	H	H	Me	H	H	-C₆H₁₁	342	0.83
175	H	H	Me	H	H	-CH(CH₃)₂	1410	0.37
176	H	H	Me	H	H	-NHCH(CH₃)₂	3570	0.10
177	Cl	H	H	H	Cl	-C₆H₁₁	150	0.12
178	Cl	H	H	H	Cl	-CH(CH₃)₂	195	0.14
179	Cl	H	H	H	Cl	-NHCH(CH₃)₂	216	0.15
180	H	Cl	H	H	H	-C₆H₁₁	165	1.41
181	H	Cl	H	H	H	-CH(CH₃)₂	164	1.09
182	H	Cl	H	H	H	-NHCH(CH₃)₂	339	0.59
183	H	CF₃	H	CF₃	H	-C₆H₁₁	1470	0.15
184	H	CF₃	H	CF₃	H	-CH(CH₃)₂	1950	0.13
185	H	CF₃	H	CF₃	H	-NHCH(CH₃)₂	1830	0.13
186	H	CF₃	H	H	H	-C₆H₁₁	937	0.35
187	H	CF₃	H	H	H	-CH(CH₃)₂	267	0.70
188	H	CF₃	H	H	H	-NHCH(CH₃)₂	932	0.31
189	F	H	H	H	F	-C₆H₁₁	174	0.94
190	F	H	H	H	F	-CH(CH₃)₂	108	0.79
191	F	H	H	H	F	-NHCH(CH₃)₂	4020	0.21
192	F	H	H	H	H	-C₆H₁₁	64	1.41
193	F	H	H	H	H	-CH(CH₃)₂	70	1.17
194	F	H	H	H	H	-NHCH(CH₃)₂	431	0.69
195	Me	H	Me	H	Me	-C₆H₁₁	518	0.24
196	Me	H	Me	H	Me	-CH(CH₃)₂	149	0.30
197	Me	H	Me	H	Me	-NHCH(CH₃)₂	431	0.14
121	H	H	H	H	H	-C₆H₁₁	36	1.55
198	H	H	H	H	H	-CH(CH₃)₂	65	1.33
200	H	H	H	H	H	-NHCH(CH₃)₂	119	1.38
201	H	F	H	H	H	-C₆H₁₁	86	1.36
202	H	F	H	H	H	-CH(CH₃)₂	71	1.33
203	H	F	H	H	H	-NHCH(CH₃)₂	467	0.61
204	H	H	F	H	H	-C₆H₁₁	185	0.53
205	H	H	F	H	H	-CH(CH₃)₂	120	1.19
206	H	H	F	H	H	-NHCH(CH₃)₂	348	0.91

	R¹	R²	R³	R⁴	R⁵	R⁶	EC₅₀ (nM)	REᵃ
213	H	F	F	H	H	-C₆H₁₁	72	1.70
214	H	F	F	H	H	-CH(CH₃)₂	249	1.15
215	H	F	F	H	H	-NHCH(CH₃)₂	8180	0.23
125	H	H	SMe	H	H	-C₆H₁₁	69	1.74
216	H	H	SMe	H	H	-CH(CH₃)₂	51	0.98
217	H	H	SMe	H	H	-NHCH(CH₃)₂	178	0.23
218	OMe	H	H	H	H	-C₆H₁₁	359	0.49
219	OMe	H	H	H	H	-CH(CH₃)₂	377	0.28
220	OMe	H	H	H	H	-NHCH(CH₃)₂	4010	0.09
126	H	Cl	H	Cl	H	-C₆H₁₁	284	0.95
221	H	Cl	H	Cl	H	-CH(CH₃)₂	661	0.54
222	H	Cl	H	Cl	H	-NHCH(CH₃)₂	>10000	0.10
223	H	OMe	H	H	H	-C₆H₁₁	101	1.51
224	H	OMe	H	H	H	-CH(CH₃)₂	72	1.26
225	H	OMe	H	H	H	-NHCH(CH₃)₂	1370	0.41
226	H	OEt	H	H	H	-C₆H₁₁	147	1.37
227	H	OEt	H	H	H	-CH(CH₃)₂	173	1.03
228	H	OEt	H	H	H	-NHCH(CH₃)₂	2350	0.33
229	H	H	OMe	H	H	-C₆H₁₁	89	1.71
230	H	H	OMe	H	H	-CH(CH₃)₂	97	1.21
231	H	H	OMe	H	H	-NHCH(CH₃)₂	144	1.16
232	H	Cl	H	H	H	-C₆H₁₁	94	1.56
233	H	Cl	H	H	H	-CH(CH₃)₂	77	1.52
234	H	Cl	H	H	H	-NHCH(CH₃)₂	1400	0.49
235	H	H	Me	H	H	-C₆H₁₁	26	1.38
236	H	H	Me	H	H	-CH(CH₃)₂	118	1.48
237	H	H	Me	H	H	-NHCH(CH₃)₂	449	0.80
238	H	Me	H	H	H	-C₆H₁₁	109	1.43
239	H	Me	H	H	H	-CH(CH₃)₂	163	1.09
240	H	Me	H	H	H	-NHCH(CH₃)₂	1330	0.53
241	OMe	H	H	Cl	H	-C₆H₁₁	233	1.16
242	OMe	H	H	Cl	H	-CH(CH₃)₂	226	0.79
243	OMe	H	H	Cl	H	-NHCH(CH₃)₂	3080	0.17
244	H	-OCH₂O-		H	H	-C₆H₁₁	38	1.90
245	H	-OCH₂O-		H	H	-CH(CH₃)₂	19	1.25
246	H	-OCH₂O-		H	H	-NHCH(CH₃)₂	96	1.51
247	H	Cl	F	H	H	-C₆H₁₁	66	1.87
248	H	Cl	F	H	H	-CH(CH₃)₂	129	1.64
249	H	Cl	F	H	H	-NHCH(CH₃)₂	3050	0.41
250	H	H	OCF₃	H	H	-C₆H₁₁	264	1.04
251	H	H	OCF₃	H	H	-CH(CH₃)₂	219	0.78
252	H	H	OCF₃	H	H	-NHCH(CH₃)₂	7530	0.21
253	H	OCF₃	H	H	H	-C₆H₁₁	420	0.84
254	H	OCF₃	H	H	H	-CH(CH₃)₂	247	0.69
255	H	OCF₃	H	H	H	-NHCH(CH₃)₂	>10000	0.09
256	OMe	H	H	H	OMe	-C₆H₁₁	77	0.12
257	OMe	H	H	H	OMe	-CH(CH₃)₂	95	0.10
258	OMe	H	H	H	OMe	-NHCH(CH₃)₂	561	0.10
259	H	H	NMe₂	H	H	-C₆H₁₁	25	1.72
260	H	H	NMe₂	H	H	-CH(CH₃)₂	57	1.07
261	H	H	NMe₂	H	H	-NHCH(CH₃)₂	162	1.01
262	H	H	t-Bu	H	H	-C₆H₁₁	132	1.38
263	H	H	t-Bu	H	H	-CH(CH₃)₂	343	0.59
264	H	H	t-Bu	H	H	-NHCH(CH₃)₂	262	1.02

	R	EC₅₀ (nM)	REᵃ
207	-C₆H₁₁	309	0.81
208	-CH(CH₃)₂	310	0.62
209	-NHCH(CH₃)₂	575	0.66

	R	EC₅₀ (nM)	REᵃ
210	-C₆H₁₁	227	0.53
211	-CH(CH₃)₂	228	0.32
212	-NHCH(CH₃)₂	366	0.42

prove useful for *in vivo* proof-of-concept experiments which may open new approaches to therapeutic agents for the treatment of diseases linked to cholesterol, bile acids, and their metabolism and homeostasis. Such studies will be reported in due course.

Experimental

General details

Reagents and resins were purchased at highest commercial quality and used without further purification, unless otherwise stated. Anhydrous solvents were obtained by passing them through a commercially available alumina column. All reactions were carried out under an argon atmosphere with dry solvents under anhydrous conditions, unless otherwise noted. Solution phase reactions were monitored by thin layer chromatography carried out on 0.25 mm E. Merck silica gel plates (60F-254) using UV light as visualizing agent and 7% ethanolic phosphomolybdic acid or *p*-anisaldehyde solution and heat as developing agents. E. Merck silica gel (60, particle size 0.040–0.063 mm) was used for flash column chromatography. Preparative thin-layer chromatography (PTLC) separations were carried out on 0.25 mm E. Merck silica gel plates (60F-254). All final products cleaved from solid support were characterized by LCMS. NMR spectra were recorded on Bruker DRX-600, AMX-500 or AMX-400 instruments and calibrated using residual undeuterated solvent as an internal reference. High resolution mass spectra (HRMS) were recorded on a VG ZAB-ZSE mass spectrometer under MALDI-FTMS conditions with NBA as the matrix. Representative procedures for each region of SAR and the final combinatorial library synthesized are provided below.

Representative procedure for synthesis of Region I/II analogues; synthesis of acrylate 29 (Scheme 1)

To a solution of aldehyde **60** (for synthesis see ref. 21) (50.0 mg, 0.229 mmol, 1.0 equiv.) in THF (1.0 mL) at 25 °C was added 3-bromoaniline (59.0 mg, 0.344 mmol, 1.5 equiv.) and the reaction mixture was heated to 70 °C. The solution was stirred for 4 h and cooled to ambient temperature. To the resulting mixture was added methanol (0.2 mL) and NaCNBH$_3$ (28.8 mg, 0.458 mmol, 2.0 equiv.) and heated to 70 °C for 4 h. The reaction mixture was then cooled and quenched with brine (5 mL). The reaction mixture was then concentrated and extracted with EtOAc (3 × 5 mL). The combined organic phase was dried over MgSO$_4$, filtered and concentrated and used without further purification (90% yield by crude ^{1}H NMR analysis). To a solution of the resulting secondary amine (0.206 mmol, 1.0 equiv.) in CH$_2$Cl$_2$ (1.0 mL) was added triethylamine (0.038 mL, 0.268 mmol, 1.3 equiv.), 4-DMAP (2.6 mg, 0.021 mmol, 0.1 equiv.), and cyclopropanecarbonyl chloride (28.0 mg, 0.268 mmol, 1.3 equiv.). The reaction mixture was stirred at 25 °C for 12 h and quenched with the addition of brine (5 mL). The aqueous phase was then extracted with CH$_2$Cl$_2$ (3 × 5 mL). The combined organic phase was dried over MgSO$_4$, filtered and concentrated and used without further purification (95% yield by crude ^{1}H NMR analysis). To the resulting amide (0.196 mmol, 1.0 equiv.) in *N*,*N*-dimethylformamide (1.0 mL) was added triethylamine (0.137 mL, 0.980 mmol, 5.0 equiv.), methyl acrylate (0.071 mL, 0.784 mmol, 4.0 equiv.), tri-*o*-tolylphosphine (30.0 mg, 0.098 mmol, 0.5 equiv.), and tris(dibenzylidene-acetone)dipalladium(0) (35.9 mg, 0.039 mmol, 0.2 equiv.) sequentially and heated to 90 °C. The reaction mixture was stirred for 24 h and then cooled to ambient temperature. The reaction mixture was then diluted with EtOAc (10 mL) and washed with water (3 × 5 mL) and brine (1 × 5 mL). The combined organic phase was dried over MgSO$_4$, filtered, concentrated and purified by column chromatography (silica, 0 → 30% EtOAc in hexanes) to afford **29** (70.1 mg, 80%).

29: R_f = 0.42 (silica, 25% ethyl acetate in hexane); FT-IR (neat) v_{max} 2943, 1720, 1642, 1596, 1443, 1414, 1314, 1267, 1202 cm^{-1}; ^{1}H NMR (400 MHz, CDCl$_3$) δ 7.60 (d, J = 15.8 Hz, 1 H), 7.40 (d, J = 7.6 Hz, 1 H), 7.34 (d, J = 7.6 Hz, 1 H), 7.31 (s, 1 H), 7.18 (d, J = 7.6 Hz, 1 H), 6.77 (d, J = 7.9 Hz, 1 H), 6.67 (d, J = 7.9 Hz, 1 H), 6.35 (d, J = 15.8 Hz, 1 H), 6.27 (d, J = 9.7 Hz, 1 H), 5.57 (d, J = 9.7 Hz, 1 H), 4.98 (s, 2 H), 3.80 (s, 3 H), 3.56 (s, 3 H), 1.42 (s, 6 H), 1.37–1.33 (m, 1 H), 1.10–1.05 (m, 2 H), 0.70–0.60 (m, 2 H); ^{13}C NMR (125 MHz, CDCl$_3$) δ 179.9, 167.1, 151.1, 145.1, 143.7, 143.4, 135.6, 130.8, 130.4, 130.1, 129.8, 128.0, 127.8, 127.6, 126.9, 122.2, 122.0, 120.9, 118.8, 76.4, 60.4, 51.8, 27.8, 8.7; HRMS calcd for C$_{27}$H$_{29}$NO$_5$ [M + H$^+$] 448.2118, found 448.2117.

Representative procedure for synthesis of Region III benzopyran containing analogues; synthesis of dichlorocyclopropane 102 (Scheme 2)

To a solution of **103** (50.0 mg, 0.089 mmol, 1.0 equiv.) in CHCl$_3$ (2.0 mL) at 25 °C was added NaOH (2.0 M, 0.3 mL) and adogen 464 (5.0 mg, *ca.* 0.1 equiv.). The resulting reaction mixture was stirred for 6 h and quenched with water (5 mL). The aqueous phase was then extracted with CH$_2$Cl$_2$ (3 × 5 mL). The combined organic phase was dried over MgSO$_4$, filtered and concentrated and used without further purification (85% yield by crude ^{1}H NMR analysis). To the resulting dichlorocyclo-propane (0.073 mmol, 1.0 equiv.) in *N*,*N*-dimethylformamide (2.0 mL) was added triethylamine (0.051 mL, 0.366 mmol, 5.0 equiv.), methyl acrylate (0.026 mL, 0.292 mmol, 4.0 equiv.), tri-*o*-tolylphosphine (11.1 mg, 0.037 mmol, 0.5 equiv.), and tris-(dibenzylideneacetone)dipalladium(0) (13.4 mg, 0.015 mmol, 0.2 equiv.) sequentially and heated to 90 °C. The reaction mixture was stirred for 24 h and then cooled to ambient temper-

ature. The reaction mixture was then diluted with EtOAc (10 mL) and washed with water (3 × 5 mL) and brine (1 × 5 mL). The combined organic phase was dried over MgSO$_4$, filtered, concentrated and purified by column chromatography (silica, 0 → 30% EtOAc in hexanes) to afford **102** (30.9 mg, 75%).

102: R_f = 0.38 (silica, 25% ethyl acetate in hexane); FT-IR (neat) v_{max} 2943, 1719, 1640, 1590, 1443, 1378, 1314, 1226, 1161 cm^{-1}; ^{1}H NMR (400 MHz, CDCl$_3$) δ 7.44 (d, J = 16.2 Hz, 1 H), 7.34 (d, J = 7.0 Hz, 1 H), 7.24–7.08 (m, 5 H), 7.04–6.98 (m, 3 H), 6.94 (d, J = 7.3 Hz, 1 H), 6.17 (d, J = 16.1 Hz, 1 H), 5.23–5.15 (m, 2 H), 3.78 (s, 3 H), 3.61 (s, 3 H), 2.84 (d, J = 10.9 Hz, 1 H), 2.06 (d, J = 10.9 Hz, 1 H), 1.72 (s, 3 H), 1.16 (s, 3 H); ^{13}C NMR (125 MHz, CDCl$_3$) δ 170.7, 167.0, 147.5, 144.1, 144.0, 143.6, 135.8, 135.1, 130.3, 129.8, 129.4, 129.3, 128.6, 128.0, 127.9, 127.8, 127.6, 127.0, 126.1, 124.8, 121.0, 118.8, 118.7, 71.4, 62.0, 60.6, 51.8, 40.9, 31.0, 27.0, 26.7; HRMS calcd for C$_{31}$H$_{29}$Cl$_2$NO$_5$ [M + Na$^+$] 588.1315, found 588.1323.

Representative procedure for synthesis of Region III non-benzo-pyran containing analogues; synthesis of bis-cinnamate 105 (Scheme 3)

To a solution of 3-bromoaniline (**130**, 60.0 mg, 0.349 mmol, 1.0 equiv.) in CH$_2$Cl$_2$ (1.0 mL) at 25 °C was added triethyl-amine (0.064 mL, 0.453 mmol, 1.3 equiv.), 4-DMAP (2.1 mg, 0.017 mmol, 0.05 equiv.), and cyclohexanecarbonyl chloride (56.3 mg, 0.384 mmol, 1.1 equiv.). The reaction mixture was stirred for 3 h and quenched with brine (5 mL). The aqueous phase was extracted with CH$_2$Cl$_2$ (3 × 5 mL) and subsequently dried over MgSO$_4$, filtered, concentrated to afford amide **131** (95% yield by crude ^{1}H NMR analysis) which was utilized without further purification. To a solution of amide **131** (0.332 mmol, 1.0 equiv.) in *N*,*N*-dimethylformamide (2.0 mL) was added triethylamine (0.232 mL, 1.66 mmol, 5.0 equiv.), methyl acrylate (0.119 mL, 1.33 mmol, 4.0 equiv.), tri-*o*-tolylphosphine (60.8 mg, 0.199 mmol, 0.6 equiv.), and tris(dibenzylidene-acetone)dipalladium(0) (60.8 mg, 0.066 mmol, 0.2 equiv.) and heated to 90 °C. The reaction mixture was stirred for 24 h and then cooled to ambient temperature. The reaction mixture was then diluted with EtOAc (15 mL) and washed with water (3 × 5 mL) and brine (1 × 5 mL). The combined organic phase was dried over MgSO$_4$, filtered, concentrated and purified by column chromatography (silica, 0 → 50% EtOAc in hexanes) to afford **132** (71.6 mg, 75%). To a solution of acrylate **132** (60.0 mg, 0.209 mmol, 1.0 equiv.) in THF (1.0 mL) at 0 °C was added NaH (9.2 mg, 0.230 mmol, 60% dispersion in mineral oil, 1.1 equiv.) followed by 4-bromobenzyl bromide (67.9 mg, 0.272 mmol, 1.3 equiv.). The reaction mixture was stirred for 2 h and quenched with saturated NH$_4$Cl (5 mL). The aqueous phase was extracted with EtOAc (3 × 5 mL) and the combined organic phase was dried over MgSO$_4$, filtered, concentrated and purified by column chromatography (silica, 0 → 30% EtOAc in hexanes) to afford **112** (85.8 mg, 90%). To a solution of amide **112** (50.0 mg, 0.110 mmol, 1.0 equiv.) in *N*,*N*-di-methylformamide (2.0 mL) was added triethylamine (0.077 mL, 0.550 mmol, 5.0 equiv.), *tert*-butyl acrylate (0.064 mL, 0.440 mmol, 4.0 equiv.), tri-*o*-tolylphosphine (5.0 mg, 0.017 mmol, 0.15 equiv.), and tris(dibenzylideneacetone)-dipalladium(0) (5.0 mg, 0.006 mmol, 0.05 equiv.) and heated to 90 °C. The reaction mixture was stirred for 12 h and then cooled to ambient temperature. The reaction mixture was then diluted with EtOAc (5 mL) and washed with water (3 × 5 mL) and brine (1 × 5 mL). The combined organic phase was dried over MgSO$_4$, filtered, concentrated and purified by column chromatography (silica, 0 → 50% EtOAc in hexanes) to afford **105** (fexaramate, 41.5 mg, 75%).

105: R_f = 0.40 (silica, 25% ethyl acetate in hexane); FT-IR (neat) v_{max} 2977, 2931, 2855, 1713, 1640, 1483, 1446, 1393, 1367, 1323, 1279, 1209 cm^{-1}; ^{1}H NMR (600 MHz, CDCl$_3$) δ 7.55 (d,

$J = 15.8$ Hz, 1 H), 7.50 (d, $J = 16.2$ Hz, 1 H), 7.44 (d, $J = 7.4$ Hz, 1 H), 7.37 (d, $J = 7.9$ Hz, 2 H), 7.32 (t, $J = 7.9$ Hz, 1 H), 7.13 (d, $J = 7.9$ Hz, 2 H), 7.05 (s, 1 H), 6.93 (d, $J = 7.0$ Hz, 1 H), 6.29 (d, $J = 16.3$ Hz, 1 H), 4.82 (s, 2 H), 3.76 (s, 3 H), 2.12–2.06 (m, 1 H), 1.68–1.60 (m, 4 H), 1.57–1.50 (m, 3 H), 1.48 (s, 9 H), 1.17–1.10 (m, 1 H), 0.97–0.89 (m, 2 H); ^{13}C NMR (150 MHz, CDCl$_3$) δ 175.9, 166.8, 166.1, 143.2, 142.9, 139.4, 135.8, 133.7, 130.0, 129.8, 129.0, 127.9, 127.6, 127.2, 120.0, 119.0, 80.3, 60.6, 52.4, 51.7, 46.6, 41.5, 31.4, 28.0, 25.3; HRMS calcd for C$_{31}$H$_{37}$NO$_5$ [M + H$^+$] 504.2744, found 504.2764.

General procedure for the solid phase synthesis of 93-membered library of biaryl and stilbene cinnamates (compounds 121, 125, 126, 174–212, and 213–264, Scheme 4)

This library was constructed *via* directed split-and-pool techniques using IRORI MacroKans™. The microreactors were initially filled with commercially availabe Merrifield resin (110 mg, 0.91 mmol g^{-1}). After encoding, all 93 microreactors were suspended in *N,N*-dimethylformamide (900 mL) and treated with Boc-protected cinnamic acid 168 (4.94 g, 18.8 mmol, 2.0 equiv.), CsCO$_3$ (6.13 g, 18.8 mmol, 2.0 equiv.), and TBAI (1.73 g, 4.7 mmol, 0.5 equiv.) and heated to 55 °C. After 24 h, the reaction mixture was cooled to ambient temperature and the reaction solvent was decanted prior to washing the microreactors with MeOH (3 × 500 mL), CH$_2$Cl$_2$ (3 × 500 mL), and Et$_2$O (3 × 500 mL). Subsequently all microreactors were pooled and suspended in CH$_2$Cl$_2$ (1000 mL) at 25 °C and treated with trifluoroacetic acid (200 mL). After 1 h, the reaction mixture was quenched with Et$_3$N (200 mL) and the reaction solvent was decanted prior to washing the microreactors with MeOH (3 × 500 mL), CH$_2$Cl$_2$ (3 × 500 mL), and Et$_2$O (3 × 500 mL). The microreactors were then pooled and resuspended in THF–MeOH (2 : 1, 1000 mL) at 25 °C and treated with 4-bromo-benzaldehyde (17.4 g, 94.0 mmol, 10.0 equiv.) and acetic acid (30 mg, 0.47 mmol, 0.05 equiv.). After 1 h, NaCNBH$_3$ (4.72 g, 75.2 mmol, 8.0 equiv.) was added and the resulting reaction was stirred a further 2 h. The reaction solvent was then decanted and the microreactors were washed with MeOH (3 × 500 mL), CH$_2$Cl$_2$ (3 × 500 mL), and Et$_2$O (3 × 500 mL).

At this point the microreactors were sorted into one of three reaction vessels and subjected to one of two acylation protocols. The microreactors of two of the reaction vessels were suspended in CH$_2$Cl$_2$ (500 mL) at 25 °C and treated with either cyclohexanecarbonyl or isobutyryl chloride (94.0 mmol, 30.0 equiv.), Et$_3$N (17.4 mL, 124 mmol, 40.0 equiv.), and 4-DMAP (380 mg, 3.1 mmol, 1.0 equiv.) and stirred for 12 h. The microreactors of the remaining reaction vessel were suspended in *N,N*-dimethylformamide (350 mL) and treated with iso-propyl isocyanate (8.0 g, 94.0 mmol, 30.0 equiv.), Et$_3$N (17.4 mL, 124 mmol, 40.0 equiv.), and 4-DMAP (380 mg, 3.1 mmol, 1.0 equiv.), heated to 60 °C and stirred for 60 h. The microreactors were then cooled and the reaction solvent was decanted prior to washing the microreactors with MeOH (3 × 500 mL), CH$_2$Cl$_2$ (3 × 500 mL), and Et$_2$O (3 × 500 mL). The microreactors were then sorted into one of 31 reaction vessels to be treated with either one of 13 commercially available styrenes or one of 18 commercially available boronic acids. For Heck coulings: The microreactors were suspended in *N,N*-dimethylformamide (100 mL) and treated with a stryrene (2.4 mmol, 8.0 equiv., see Fig. S-15† for the identities of styrenes), Et$_3$N (0.42 mL, 3.0 mmol, 10.0 equiv.), tri-*o*-tolyl-phosphine (138 mg, 0.45 mmol, 1.5 equiv.), and tris(dibenzyl-ideneacetone)dipalladium(0) (138 mg, 0.15 mmol, 0.5 equiv.) and heated to 90 °C for a period of 48 h. For Suzuki couplings: The microreactors were suspended in *N,N*-dimethylformamide (100 mL) and treated with a boronic acid (2.4 mmol, 8.0 equiv., see Fig. S-15† for the identities of boronic acids), CsCO$_3$ (293 mg, 0.9 mmol, 3.0 equiv.), and tetrakis(triphenylphos-phine)palladium(0) (173 mg, 0.15 mmol, 0.5 equiv.) and heated

to 90 °C for a period of 24 h. The microreactors were then pooled and the reaction solvent was decanted prior to washing the microreactors with MeOH (3 × 500 mL), CH$_2$Cl$_2$ (3 × 500 mL), and Et$_2$O (3 × 500 mL). Finally, each microreactor was sorted into an individual reaction vessel and cleaved upon suspension in Et$_2$O and subsequent treatment with a solution of NaOMe in MeOH (approx. 10 equiv.) at 25 °C for a period of 20 min. The reactions were quenched with brine, extracted with Et$_2$O, concentrated and each compound was purified by preparatory thin layer chromatography (PTLC). Each compound was analyzed using LCMS which gave an average purity of 95% for the library and 93/93 parent mass peaks found. LCMS traces along with the corresponding mass spectra are available upon request.

Full characterization of representative members of the four classes of potent, selective FXR agonists (Fig. 9)

128: R_f = 0.43 (silica, 25% ethyl acetate in hexane); FT-IR (neat) v_{max} 3058, 2927, 2854, 1715, 1642, 1598, 1588, 1483, 1435, 1398, 1318, 1271, 1230, 1201 cm^{-1}; ^{1}H NMR (600 MHz, CDCl$_3$) δ 7.58 (d, $J = 15.8$ Hz, 1 H) 7.44 (d, $J = 7.4$ Hz, 1 H), 7.42 (d, $J = 7.9$ Hz, 2 H), 7.31 (t, $J, = 7.9$ Hz, 1 H), 7.13 (s, 1 H), 7.12 (s, 2 H), 7.05 (d, $J = 3.1$ Hz, 1 H), 6.96 (d, $J = 7.0$ Hz, 1 H), 6.67 (d, $J = 2.6$ Hz, 1 H), 6.33 (d, $J = 16.2$ Hz, 1 H), 4.83 (s, 2 H), 3.76 (s, 3 H), 2.46 (s, 3 H), 2.16–2.07 (m, 1 H), 1.70–1.64 (m, 4 H), 1.62–1.48 (m, 3 H), 1.20–1.11 (m, 1 H), 0.99–0.92 (m, 2 H); ^{13}C NMR (150 MHz, CDCl$_3$) δ 175.8, 166.8, 143.3, 143.0, 141.4, 139.3, 136.1, 135.8, 133.7, 129.9, 129.0, 127.1, 126.0, 125.3, 122.7, 118.9, 60.5, 52.3, 51.6, 41.5, 29.4, 25.4, 25.2, 15.3, 14.0; HRMS calcd for C$_{29}$H$_{31}$NO$_3$S [M + Na$^+$] 496.1917, found 496.1924.

121: R_f = 0.35 (silica, 25% ethyl acetate in hexane); FT-IR (neat) v_{max} 2928, 2854, 1717, 1646, 1597, 1578, 1508, 1489, 1448, 1397, 1318, 1268, 1200 cm^{-1}; ^{1}H NMR (400 MHz, CDCl$_3$) δ 7.60 (d, $J = 16.1$ Hz, 1 H), 7.49 (d, $J = 7.4$ Hz, 2 H), 7.47–7.43 (m, 1 H), 7.41 (d, $J = 7.9$ Hz, 2 H), 7.34 (t, $J = 7.6$ Hz, 3 H), 7.24 (t, $J = 7.3$ Hz, 1 H), 7.15 (d, $J = 7.9$ Hz, 1 H), 7.11–7.07 (m, 3 H), 6.98 (d, $J = 7.0$ Hz, 1 H), 6.34 (d, $J = 16.1$ Hz, 1 H), 4.86 (s, 2 H), 3.79 (s, 3 H), 2.17–2.10 (m, 1 H), 1.71–1.52 (m, 7 H), 1.22–1.14 (m, 1 H), 1.00–0.88 (m, 2 H); ^{13}C NMR (100 MHz, CDCl$_3$) δ 176.0, 167.0, 143.5, 143.1, 137.3, 137.0, 136.5, 135.9, 130.0, 129.1, 128.6, 128.2, 127.8, 127.6, 127.3, 126.5, 126.4, 119.1, 60.7, 52.5, 51.8, 41.7, 29.5, 25.6, 25.4, 14.3; HRMS calcd for C$_{32}$H$_{33}$NO$_3$ [M + H$^+$] 480.2533, found 480.2534.

210: R_f = 0.10 (silica, 25% ethyl acetate in hexane); FT-IR (neat) v_{max} 2930, 1715, 1644, 1530, 1446, 1398, 1318, 1174 cm^{-1}; ^{1}H NMR (400 MHz, CDCl$_3$) δ 7.58 (d, $J = 16.2$ Hz, 1 H), 7.46 (d, $J = 7.3$ Hz, 1 H), 7.39–7.26 (m, 3 H), 7.17–7.07 (m, 4 H), 6.97 (d, $J = 6.8$ Hz, 1 H), 6.76 (d, $J = 16.2$ Hz, 1 H), 6.32 (d, $J = 16.1$ Hz, 1 H), 4.84 (s, 2 H), 3.76 (s, 3 H), 2.51 (s, 3 H), 2.14–2.06 (m, 1 H), 1.70–1.50 (m, 7 H), 1.22–1.12 (m, 1 H), 1.00–0.85 (m, 2 H); ^{13}C NMR (100 MHz, CDCl$_3$) δ 176.0, 167.0, 150.5, 149.5, 143.4, 143.1, 137.4, 135.9, 132.9, 132.0, 131.8, 130.8, 130.0, 129.2, 127.8, 127.2, 126.4, 119.1, 118.2, 60.7, 52.5, 51.8, 41.7, 29.4, 25.5, 15.4; HRMS calcd for C$_{30}$H$_{32}$N$_2$O$_3$S [M + H$^+$] 501.2206, found 501.2202.

125: R_f = 0.33 (silica, 25% ethyl acetate in hexane); FT-IR (neat) v_{max} 3025, 2926, 2854, 1714, 1643, 1597, 1580, 1488, 1435, 1394, 1359, 1318, 1269, 1231, 1202 cm^{-1}; ^{1}H NMR (600 MHz, CDCl$_3$) δ 7.59 (d, $J = 16.2$ Hz, 1 H), 7.52–7.44 (m, 5 H), 7.35 (t, $J = 7.4$ Hz, 1 H), 7.28 (d, $J = 8.3$ Hz, 2 H), 7.21 (d, $J = 8.3$ Hz, 2 H), 7.12 (br s, 1 H), 7.01 (d, $J = 7.0$ Hz, 1 H), 6.32 (d, $J = 16.2$ Hz, 1 H), 4.88 (s, 2 H), 3.77 (s, 3 H), 2.49 (s, 3 H), 2.16–2.11 (m, 1 H), 1.70–1.65 (m, 3 H), 1.62–1.50 (m, 4 H), 1.20–1.15 (m, 1 H), 0.96–0.90 (m, 2 H); ^{13}C NMR (150 MHz, CDCl$_3$) δ 175.9, 166.9, 143.3, 143.0, 139.4, 137.5, 137.4, 136.4, 135.8, 129.9, 129.7, 129.0, 127.6, 127.2, 126.8, 126.7, 119.0, 60.6, 52.4, 51.7, 41.6, 29.4, 25.4, 25.3, 15.7; HRMS calcd for C$_{31}$H$_{33}$NO$_3$S [M + Na$^+$] 522.2073, found 522.2053.

192: R_f = 0.35 (silica, 25% ethyl acetate in hexane); FT-IR (neat) v_{max} 2928, 2854, 1716, 1652, 1508, 1485, 1449, 1397, 1318, 1268, 1231, 1200 cm^{-1}; ^{1}H NMR (400 MHz, CDCl$_3$) δ 7.59 (d, J = 16.7 Hz, 1 H), 7.56–7.53 (m, 1 H), 7.45 (d, J = 7.6 Hz, 1 H), 7.41 (d, J = 7.9 Hz, 2 H), 7.33 (t, J = 1 Hz), 7.22–7.06 (m, 7 H), 7.06–6.94 (m, 2 H), 6.33 (d, J = 16.1 Hz, 1 H), 4.85 (s, 2 H), 3.76 (s, 3 H), 2.17–2.09 (m, 1 H), 1.72–1.50 (m, 7 H), 1.21–1.12 (m, 1 H), 1.00–0.88 (m, 2 H); ^{13}C NMR (100 MHz, CDCl$_3$) δ 176.0, 167.0, 161.6, 159.1, 143.4, 137.3, 136.4, 135.9, 130.4, 130.0, 129.1, 128.8, 127.7, 127.3, 127.0, 125.2, 125.0, 124.1, 120.8, 119.1, 115.9, 115.6, 52.5, 51.8, 41.7, 29.5, 25.6, 25.4, 14.2; HRMS calcd for C$_{32}$H$_{32}$FNO$_3$ [M + H$^+$] 498.2439, found 498.2450.

259: R_f = 0.27 (silica, 25% ethyl acetate in hexane); FT-IR (neat) v_{max} 2928, 1716, 1646, 1609, 1579, 1539, 1504, 1446, 1396, 1357, 1319, 1268 cm^{-1}; ^{1}H NMR (400 MHz, CDCl$_3$) δ 7.61 (d, J = 15.8 Hz, 1 H), 7.51–7.41 (m, 5 H), 7.35 (t, J = 7.6 Hz, 1 H), 7.17 (d, J = 7.9 Hz, 2 H), 7.13 (br s, 1 H), 7.00 (d, J = 7.0 Hz, 1 H), 6.79 (d, J = 7.9 Hz, 2 H), 6.34 (d, J = 16.1 Hz, 1 H), 4.87 (s, 2 H), 3.79 (s, 3 H), 2.99 (s, 6 H), 2.18–2.10 (m, 1 H), 1.70–1.50 (m, 7 H), 1.22–1.15 (m, 1 H), 1.00–0.90 (m, 2 H); ^{13}C NMR (100 MHz, CDCl$_3$) δ 175.9, 167.0, 143.5, 143.2, 140.2, 135.9, 135.2, 130.1, 130.0, 129.1, 127.8, 127.6, 127.2, 126.2, 119.0, 112.7, 60.7, 52.5, 51.8, 41.7, 40.6, 29.5, 25.6, 25.5, 14.3; HRMS calcd for C$_{32}$H$_{36}$N$_2$O$_3$ [M + $^{\cdot}$] 496.2720, found 496.2715.

244: R_f = 0.25 (silica, 25% ethyl acetate in hexane); FT-IR (neat) v_{max} 2930, 2855, 1716, 1652, 1599, 1579, 1504, 1486, 1445, 1398, 1318, 1226 cm^{-1}; ^{1}H NMR (400 MHz, CDCl$_3$) δ 7.60 (d, J = 16.2 Hz, 1 H), 7.46 (d, J= 7.6 Hz, 1 H), 7.40 (d, J = 7.9 Hz, 2 H), 7.35 (t, J = 8.0 Hz, 1 H), 7.18 (d, J = 7.9 Hz, 2 H), 7.10 (br s, 1 H), 7.05–7.00 (m, 3 H), 6.84 (d, J = 7.6 Hz, 1 H), 6.31 (d, J = 15.8 Hz, 1 H), 5.96 (s, 2 H), 4.87 (s, 2 H), 3.78 (s, 3 H), 2.19–2.10 (m, 1 H), 1.70–1.50 (m, 7 H), 1.25–1.15 (m, 1 H), 1.00–0.90 (m, 2 H); ^{13}C NMR (100 MHz, CDCl$_3$) δ 176.0, 167.0, 148.0, 147.0, 143.5, 143.1, 140.0, 136.2, 135.9, 130.1, 130.0, 127.7, 127.4, 126.9, 120.5, 119.0, 108.5, 107.6, 101.1, 52.5, 51.8, 41.7, 29.5, 25.6, 25.4; HRMS calcd for C$_{31}$H$_{31}$NO$_5$ [M + H$^+$] 498.2275, found 498.2269.

149: R_f = 0.25 (silica, 25% ethyl acetate in hexane); FT-IR (neat) v_{max} 2932, 1720, 1642, 1580, 1454, 1399, 1341, 1318, 1269, 1202 cm^{-1}; ^{1}H NMR (400 MHz, CDCl$_3$) δ 7.52 (d, J = 16.1 Hz, 1 H), 7.39 (d, J = 7.0 Hz, 1 H), 7.29 (t, J = 7.4 Hz, 1 H), 7.02 (br s, 2 H), 6.96 (d, J = 7.6 Hz, 1 H), 6.83 (d, J = 7.0 Hz, 1 H), 6.28 (d, J = 16.1 Hz, 1 H), 4.95–4.85 (m, 2 H), 3.78 (s, 3 H), 3.39 (s, 3 H), 2.81 (d, J = 10.8 Hz, 1 H), 2.15 (d, J = 10.8 Hz, 1 H), 2.15–2.05 (m, 1 H), 1.67 (s, 6 H), 1.60–1.49 (3 H), 1.25–1.10 (m, 5 H), 1.00–0.85 (m, 2 H); ^{13}C NMR (100 MHz, CDCl$_3$) δ 176.0, 166.9, 147.6, 144.0, 143.5, 143.0, 135.6, 130.4, 130.0, 129.8, 127.8, 127.3, 124.8, 121.5, 118.9, 118.6, 71.3, 62.0, 60.4, 51.8, 46.4, 41.7, 40.9, 31.0, 29.5, 29.4, 26.9, 26.6, 25.6, 25.4; HRMS calcd for C$_{31}$H$_{35}$Cl$_2$NO$_5$ [M + Na$^+$] 594.1784, found 594.1790.

Acknowledgements

References

1 R. W. Mahley and T. P. Bersot, in *The Pharmacological Basis of Therapeutics*, eds. L. S. Goodman and A. Z. Gilman, McGraw Hill, New York, 1996, 9th edition, ch. 36.

2 A. Chawia, E. Saez and R. M. Evans, *Cell*, 2000, **103**, 1–4.

3 H. Tu, A. Y. Okamoto and T. Hua, *Trends Cardiovasc. Med.*, 2000, **10**, 30–35.

4 T. T. Lu, J. J. Repa and D. J. Mangelsdorf, *J. Biol. Chem.*, 2001, **276**, 37735–37738.

5 P. A. Edwads, H. R. Kast and A. M. Anisfeld, *J. Lipid. Res.*, 2002, **43**, 2–12.

6 M. Makishima, A. Y. Okamoto, J. J. Repa, H. Tu, R. M. Learned, A. Luk, M. V. Hull, K. D. Lustig, D. J. Mangelsdorf and B. Shan, *Science*, 1999, **284**, 1362–1365.

7 D. J. Parks, S. G. Blanchard, R. K. Bledsoe, G. Chandra, T. G. Consler, S. A. Kliewer, J. B. Stimmel, T. M. Willson, A. M. Zavacki, D. D. Moore and J. M. Lehmann, *Science*, 1999, **284**, 1365–1368.

8 H. Wang, J. Chen, K. Hollister, L. C. Sowers and B. M. Forman, *Mol. Cell*, 1999, **3**, 543–553.

9 B. Goodwin, S. A. Jones, R. R. Price, M. A. Watson, D. D. McKee, L. B. Moore, C. Galardi, J. G. Wilson, M. C. Lewis, M. E. Roth, P. R. Maloney, T. M. Willson and S. A. Kliewer, *Mol. Cell*, 2000, **6**, 517–526.

10 T. Lu, M. Makishima, J. J. Repa, K. Schoonjans, T. A. Kerr, J. Auwerx and D. J. Mangelsdorf, *Mol. Cell*, 2000, **6**, 507–515.

11 H. R. Kast, C. M. Nguyen, C. J. Sinal, S. A. Jones, B. A. Laffitte, K. Reue, F. J. Gonzalez, T. M. Willson and P. A. Edwards, *Mol. Endocrin.*, 2001, **15**, 1720–1728.

12 C. S. Song, I. Echchgadda, B.-S. Baek, S. C. Ahn, T. Oh, A. K. Roy and B. Chatterjee, *J. Biol. Chem.*, 2001, **276**, 42549–42556.

13 H. R. Kast, B. Goodwin, P. T. Tarr, S. A. Jones, A. M. Anisfeld, C. M. Stolz, P. Tontonoz, S. Kliewer, T. M. Willson and P. A. Edwards, *J. Biol. Chem.*, 2002, **277**, 2908–2915.

14 M. Ananthanarayanan, N. Balasubramanian, M. Makishima, D. J. Mangelsdorf and F. J. Suchy, *J. Biol. Chem.*, 2001, **276**, 28857–28865.

15 B. A. Laffitte, H. R. Kast, C. M. Nguyen, A. M. Zavacki, D. D. Moore and P. A. Edwards, *J. Biol. Chem.*, 2000, **275**, 10638–10647.

16 N. L. Urizar, D. H. Dowhan and D. D. Moore, *J. Biol. Chem.*, 2000, **275**, 39313–39317.

17 J. Grober, I. Zaghini, H. Fujii, S. A. Jones, S. A. Kliewer, T. M. Willson, T. Ono and P. Besnard, *J. Biol. Chem.*, 1999, **274**, 29749–29754.

18 T. M. Willson, S. A. Jones, J. T. Moore and S. A. Kliewer, *Med. Res. Rev.*, 2001, **21**, 513–522.

19 P. R. Maloney, D. J. Parks, C. D. Haffner, A. M. Fivush, G. Chandra, K. D. Plunket, K. L. Creech, L. B. Moore, J. G. Wilson, M. C. Lewis, S. A. Jones and T. M. Willson, *J. Med. Chem.*, 2000, **43**, 2971–2974.

20 For another potent steroid-derived agonist of FXR see: R. Pellicciari, S. Fiorucci, E. Camaioni, C. Clerici, G. Costantino, P. R. Maloney, A. Morelli, D. J. Parks and T. W. Willson, *J. Med. Chem.*, 2002, **45**, 3569–3572.

21 K. C. Nicolaou, J. A. Pfefferkorn, A. J. Roecker, G.-Q. Cao, S. Barluenga and H. J. Mitchell, *J. Am. Chem. Soc.*, 2000, **122**, 9939–9953.

22 K. C. Nicolaou, J. A. Pfefferkorn, H. J. Mitchell, A. J. Roecker, S. Barluenga, G.-Q. Cao, R. L. Affleck and J. E. Lillig, *J. Am. Chem. Soc*, 2000, **122**, 9954–9967.

23 K. C. Nicolaou, J. A. Pfefferkorn, S. Barluenga, H. J. Mitchell, A. J. Roecker and G.-Q. Cao, *J. Am. Chem. Soc.*, 2000, **122**, 9968–9976.

24 K. C. Nicolaou, J. A. Pfefferkorn, F. Schuler, A. J. Roecker, G.-Q. Cao and J. E. Casida, *Chem. Biol.*, 2000, **7**, 979–992.

25 K. C. Nicolaou, A. J. Roecker, S. Barluenga, J. A. Pfefferkorn and G.-Q. Cao, *ChemBioChem*, 2001, **6**, 460–465.

26 G. J. Fraser, W. Xiang, R. Mercuri, C. Illy, B. R. Bowen, Y. He and M. Sillis, *J. Biol. Screen.*, 2002, **7**, 3–10.

27 L. Xu, C. K. Glass and M. G. Rosenfeld, *Curr. Opin. Gen. Dev.*, 1999, **9**, 140–147.

28 C. K. Glass, D. W. Rose and M. G. Rosenfeld, *Curr. Opin. Cell Biol.*, 1997, **9**, 222–232.

29 D. L. Boger, J. Hong, M. Hikota and M. Ishida, *J. Am. Chem. Soc.*, 1999, **121**, 2471–2477.

30 The lead compounds were analyzed for their ability to modulate the activity of the following nuclear receptors: RXRα, PPARα, PPARγ, PPARδ, PXR, SXR, LXRα, TRβ, RARβ, CARR, ERR3, VDR: M. Downes, M. Verdecia, A. J. Roecker, R. Hughes, J. B. Hogenesch, H. R. Kast, A. E. Bowman, J-L. Ferrer, A. M. Anisfeld, P. A. Edwards, J. M. Rosenfeld, J. G. A. Alvarez, J. P. Noel, K. C. Nicolaou and R. M. Evans, *Mol. Cell*, 2003, in press.

31 T. M. Willson and S. A. Kliewer, *J. Lipid Res.*, 2002, **43**, 359–364.

32 X. Wen, A. Radominska-Pandya, Y. Shi, C. M. Simon, M. C. Nelson, E. S. Ong, D. J. Waxman and R. M. Evans, *Proc. Natl. Acad. Sci. U.S.A.*, 2001, **98**, 3375–3380.